# 1

# Overview of Vibrational Optical Activity



## 1.1 Introduction to Vibrational Optical Activity

Vibrational optical activity (VOA) is a new form of natural optical activity whose early history dates back to the nineteenth century. We now know that the original observations of optical activity, the rotation of the plane of linearly polarized radiation, termed optical rotation (OR), or the differential absorption of left and right circularly polarized light, circular dichroism (CD), have their origins in electronic transitions in molecules. Not until after the establishment of quantum mechanics and molecular spectroscopy in the twentieth century was the physical basis of natural optical activity revealed for the first time.

### 1.1.1 Field of Vibrational Optical Activity

Vibrational optical activity, as the name implies, is the area of spectroscopy that results from the introduction of optical activity into the field of vibrational spectroscopy. VOA can be broadly defined as the difference in the interaction of left and right circularly polarized radiation with a molecule or molecular assembly undergoing a vibrational transition. This definition allows for a wide variety of spectroscopies, as will be discussed below, but the most important of these are the forms of VOA associated with infrared (IR) absorption and Raman scattering. The infrared form is known as vibrational circular dichroism, or VCD, while the Raman form is known as vibrational Raman optical activity, VROA, or usually just ROA (Raman optical activity). VCD and ROA were discovered experimentally in the early 1970s and have since blossomed independently into two important new fields of spectroscopy for probing the structure and conformation of all classes of chiral molecules and supramolecular assemblies.

VCD has been measured from approximately $600\,\mathrm{cm}^{-1}$ in the mid-infrared region, into the hydrogen stretching region and through the near-infrared region to almost the visible region of the spectrum at $14\,000\,\mathrm{cm}^{-1}$. The infrared frequency range of up to $4000\,\mathrm{cm}^{-1}$ is comprised mainly of fundamental transitions, while higher frequency transitions in the near-infrared are dominated by

*Vibrational Optical Activity: Principles and Applications*, First Edition. Laurence A. Nafie.

overtone and combination band transitions. ROA has been measured to as low as 50 $cm^{-1}$, a distinct difference compared with VCD, but ROA is more difficult to measure beyond the range of fundamental transitions and is typically only measured for vibrational transitions below 2000 $cm^{-1}$. VCD and ROA can both be measured as electronic optical activity in molecules possessing low-lying electronic states, although in the case of VCD it is appropriate to refer to these phenomena as infrared electronic circular dichroism, IR-ECD or IRCD, and electronic ROA, or EROA.

VCD and ROA are typically measured for liquid or solution-state samples. VCD has been measured in the gas phase and in the solid phase as mulls, KBr pellets and films of various types. When sampling solids, distortions of the VCD spectra due to birefringence and particle scattering need to be avoided. To date, ROA has not been measured in gases or diffuse solids, but nothing precludes this sampling option, although technical issues may arise, such as sufficient Raman intensity for gases and competing particle scattering for diffuse solids.

At present, there is only one form of VCD, namely the one-photon differential absorption form, although recently, a second manifestation of VCD, the differential refractive index, termed the called vibrational circular birefringence (VCB), has been measured. A VCB spectrum is the Kramers–Kronig transform of a VCD spectrum and is also known as vibrational optical rotatory dispersion (VORD). As we shall see, ORD is the oldest form of optical activity and the form of VOA that was sought in the 1950s and 1960s before the discovery of VCD. By comparison, ROA is much richer in experimental possibilities. Because one can consider circular (or linear) polarization differences in Raman scattering intensity associated with the incident or scattered radiation, or both, in-phase and out-of-phase, there are four (eight) distinct forms of ROA. Further, for ROA there are choices of scattering geometry and the frequency of the incident radiation, both of which give rise to different ROA spectra. As a result, there is in principle a continuum of different types of VOA measurements that can be envisioned for a given choice of sample molecule.

Beyond this, many other forms of VOA are possible. One form is reflection vibrational optical activity, which would include VCD measured as specular reflection, diffuse reflection or attenuated total reflection (ATR). In principle, VCD could also be measured in fluorescence. Because fluorescence depends on the third power of the exciting frequency, infrared fluorescence VOA would be very weak relative to VCD and thus very difficult to measure. As with fluorescence in the visible and ultraviolet regions of the spectrum, fluorescence VCD could be measured in two forms, fluorescence detected VCD or circularly polarized emission VCD. In the former, one would measure all the fluorescence intensity resulting from the differential absorbance of left and right circularly polarized infrared radiation (VCD) or measure the difference in left and right circularly polarized infrared emission from unpolarized exciting infrared radiation. Finally, we note the various manifestations of nonlinear or multi-photon VCD, such as two-photon infrared absorption VCD.

In the case of ROA there are a variety of different forms of VOA yet to be measured. One recently reported for the first time is near-infrared excited ROA. Other forms of ROA yet to be measured are ultraviolet resonance Raman ROA, surface-enhanced ROA, coherent anti-Stokes ROA, and hyper-ROA in which two laser photons generate an ROA spectrum in the region of twice the laser frequency. Second harmonic generation (SHG) ROA at two-dimensional interfaces has been measured, and attempts have been made to measure sum frequency generation (SFG) VOA, which is an interesting form of optical activity that depends on transition moments which arise in both VCD and ROA.

Another class of optical activity that has VOA content is vibronic optical activity. Here the source of optical activity is a combination of electronic optical activity (EOA) and VOA when changes to both electronic and vibrational states occur in a transition. This form of EOA–VOA arises in ECD whenever vibronic detail is observed. The analogous form of ROA is either vibronically resolved electronic ROA or ROA arising from strong resonance with particular vibronic states of a molecule.

Finally, we consider other forms of radiation that may affect vibrational transitions in molecules. In particular, it is possible to create beams of neutrons that are circular polarized either to the left or to the right. This phenomenon has been considered theoretically, but experimental attempts at measurement have not been reported. Another common form of vibrational spectroscopy that does not involve photons as the source of radiation interaction is electron energy loss spectroscopy. This is essentially Raman scattering using electrons. If modulation between left and right circularly polarized electrons could be realized, then this could become a new form of VOA in the future.

### 1.1.2 Definition of Vibrational Circular Dichroism

VCD is defined as the difference in the absorbance of left minus right circularly polarized light for a molecule undergoing a vibrational transition. For VCD to be non-zero, the molecule must be chiral or else be in a chiral molecular environment, such as a non-chiral molecule in a chiral molecular crystal or bound to a chiral molecule. The definition of VCD is illustrated in Figure 1.1 for a molecule undergoing a transition from the zeroth (0) to the first (1) vibrational level of the ground electronic state ($g$) of a molecule.

More generally, we can define VCD for a transition between any two vibrational sublevels $ev$ and $ev'$ of an electronic state $e$ as:

$$\text{VCD} \qquad (\Delta A)^{a}_{ev',ev} = (A_L)^{a}_{ev',ev} - (A_R)^{a}_{ev',ev} \tag{1.1}$$

where $A_{\mathrm{L}}$is the absorbance for left circularly polarized light and $A_{\mathrm{R}}$ is the absorbance for right circularly polarized light. The superscript $a$ refers to the vibrational mode, or modes, associated with the vibrational transition. The sense of the definition of VCD is left minus right circularly polarization in conformity with the definition used for electronic circular dichroism (ECD). The parent ordinary infrared absorption intensity associated with VCD, also referred to as vibrational absorbance (VA), is defined as the average of the individual absorbance intensities for left and right circularly polarized radiation, namely:

$$\text{VA} \qquad (A)^{a}_{ev',ev} = \frac{1}{2}\left[(A_L)^{a}_{ev',ev} + (A_R)^{a}_{ev',ev}\right] \tag{1.2}$$

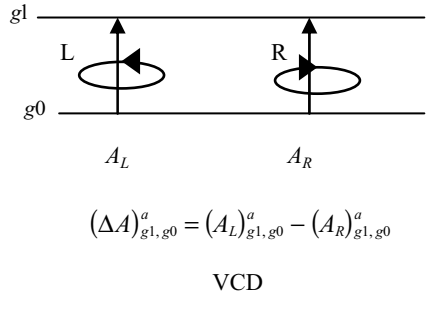


***Figure 1.1*** *Energy-level diagram illustrating the definition of VCD for a molecule undergoing a transition from the zeroth to the first vibrational level of the ground electronic state*

These definitions of VCD and VA represent the total intensity associated with a given vibrational transition with the label $a$. Experimentally, one measures VCD and VA spectra as bands in the spectrum that have a shape or distribution as a function of radiation frequency $\nu$, which is expressed as $f_a^{'}(\nu)$ for each vibrational transition. The reason for the prime will be explained in Chapter 3. An experimentally measured VCD or VA spectrum is therefore related to the defined quantities in Equations (1.1) and (1.2) by sums over all the vibrational transitions $a$ in the spectrum as:

$$\Delta A(\nu) = \sum_a (\Delta A)^a_{ev',ev} f_a^{'}(\nu) \tag{1.3}$$

$$A(\nu) = \sum_a (A)^a_{ev',ev} f_a^{'}(\nu) \tag{1.4}$$

From these expressions it can also be seen that the original definitions of VCD and VA in Equations (1.1) and (1.2) represent integrated intensities over the measured VCD, or VA, band of vibrational transition $a$ by writing for example:

$$\Delta A^a_{ev',ev} = \int_a \Delta A(\nu) \mathrm{d}\,\nu = \int_a \Delta A^a_{ev',ev} f_a^{'}(\nu) \mathrm{d}\,\nu = \Delta A^a_{ev',ev} \int_a f_a^{'}(\nu) \mathrm{d}\,\nu \tag{1.5}$$

where the last integral on the right-hand side of this expression is equal to 1 when a normalized bandshape of unit area is used as:

$$\int_a f_a^{'}(\nu) \mathrm{d}\,\nu = 1 \tag{1.6}$$

Experimentally, the VA intensities are defined by the relationship:

$$A(\nu) = -\log_{10}[I(\nu)/I_0(\nu)] = \varepsilon(\nu) bC \tag{1.7}$$

where $I(\nu)$ is the IR transmission intensity of the sample, which is divided by the reference transmission spectrum of the instrument, $I_0(\nu)$, usually without the sample in place. Normalization of the sample transmission by the reference spectrum removes the dependence of the measurement on the characteristics of the instrument used for the measurement of the spectrum, namely throughput and spectral profile. The second part of Equation (1.7) assumes Beer–Lambert's law and defines the molar absorptivity of the sample, $\varepsilon(\nu)$, where $b$ and $C$ are the pathlength and molar concentration in the case of solution-phase samples, respectively. The experimental measurement of VCD is similar, but more complex than the definition of VA in Equation (1.7), and we defer description of this definition until Chapter 6, when the measurement of VCD is described in detail. The definition of the molar absorptivity in Equation (1.7) yields a molecular-level definition of VCD intensity, $\Delta\varepsilon(\nu)$, which is free of the choice of the sampling variables pathlength and concentration. This is given by:

$$\Delta\varepsilon(\nu) = \Delta A(\nu)/(ee) bC \tag{1.8}$$

where (*ee*) is the enantiomeric excess of the sample. The (*ee*) can be defined as the concentration of the major enantiomer, $C_M$, minus that of the minor enantiomer, $C_m$, divided by the sum of their concentrations, which is also the total concentration.

$$(ee) = \frac{C_M - C_m}{C_M + C_m} = \frac{C_M - C_m}{C} \tag{1.9}$$

The value of (*ee*) can vary from unity for a sample of only a single enantiomer to zero for a racemic mixture of both enantiomers, such that neither enantiomer is in excess. Thus we can write:

$$\Delta\varepsilon(\nu) = \Delta A(\nu)/b(C_M - C_m) \tag{1.10}$$

This definition of VCD represents a molecular-level quantity that has been corrected for the pathlength and concentrations of both enantiomers. The intensity expressed as molar absorptivity of a VCD band for vibrational transition *a*, $(\Delta\varepsilon)^a_{ev',ev}$, can be extracted from the experimentally measured molar absorptivity VCD spectrum by integration over the VCD band of transition *a*, as:

$$(\Delta\varepsilon)^a_{ev',ev} = \int_a \Delta\varepsilon(\nu)\mathrm{d}\nu \tag{1.11}$$

The quantity $(\Delta\varepsilon)^a_{ev',ev}$can be compared directly with theoretical expressions of VCD intensity.

A transition between vibrational levels separated by a single quantum of vibrational energy corresponds to a fundamental transition and is described by the superscript *a* for a particular vibrational mode in the definitions above. In the case of higher level vibrational transitions, more than one vibrational quantum number is needed, such as *ab* for *a* a combination band of mode *a* and mode *b*, or *2a* for the first overtone of mode *a*. All fundamental transitions occur in the IR region below a frequency of 4000 $\mathrm{cm}^{-1}$ and all vibrational transitions above that frequency in the near-infrared region involve only overtones and combination bands.

### 1.1.3 Definition of Vibrational Raman Optical Activity

ROA is defined as the difference in Raman scattering intensity for right minus left circularly polarized incident and/or scattered radiation. There are four forms of circular polarization ROA. Energy-level diagrams are given in Figure 1.2 for a molecule undergoing a transition from the zeroth to the first vibrational level of the ground electronic state. The left-hand vertical upward-pointing arrows represent the incident laser radiation, and the right-hand downward-pointing arrows represent the scattered Raman radiation. A Stokes Raman scattering process is assumed such that the molecule gains vibrational energy while the scattering Raman radiation is red-shifted from the incident laser radiation by the same energy. The initial and final states of the Raman-ROA transitions, *g*0 and *g*1, are the same as those in Figure 1.1 for VA-VCD transitions. The excited vibrational–electronic (*ev*) states of the molecule are represented by energy levels above the energy of the incident laser radiation, which applies for the common case in which the incident radiation has lower energy than any of the allowed electronic states of the molecule.

The original form of ROA is now called incident circular polarization (ICP) ROA. Here the incident laser is modulated between right and left circular polarization states, and the Raman intensity is measured at a fixed linear or unpolarized radiation state. The second form of ROA is called scattered circular polarization (SCP) ROA. In this form, fixed linear or unpolarized incident laser radiation is used and the difference in the right and left circularly polarized Raman scattered light is measured. The third form of ROA is in-phase dual circular polarization ($\mathrm{DCP_I}$) ROA. Here the

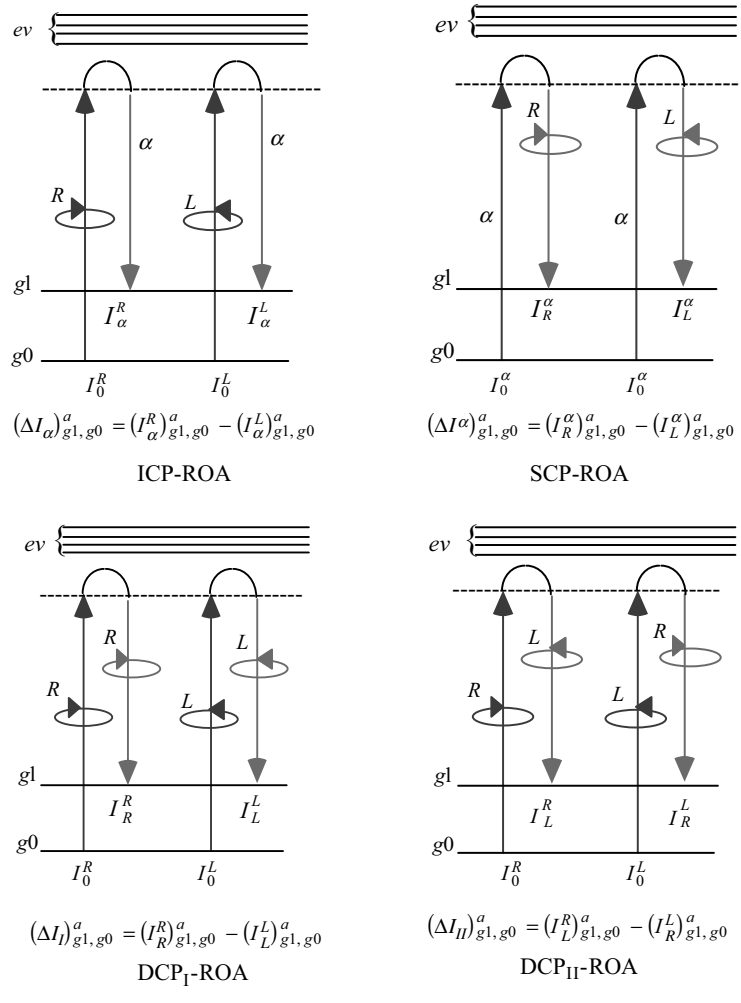


***Figure 1.2*** *Energy-level diagrams illustrating the definition of ROA for a molecule undergoing a transition from the zeroth (g0) to the first (g1) vibrational level of the ground electronic state, where the excited intermediate states of the Raman transition are represented by electronic–vibrational levels (ev)*

polarization states of both the incident and scattered radiation are switched synchronously between right and left circular states. The last form of ROA is called out-of-phase dual circular polarization ($DCP_{II}$) ROA, where the polarization states of both the incident and scattered radiation are switched oppositely between left and right circular states. The definitions of these forms of ROA for any vibrational transition involving normal mode $a$ between states $ev$ and $ev'$ are given by the following expressions.

$$\text{ICP ROA} \quad (\Delta I_\alpha)^a_{ev',ev} = (I_\alpha^R)^a_{ev',ev} - (I_\alpha^L)^a_{ev',ev} \tag{1.12a}$$

$$\text{SCP ROA} \quad (\Delta I^\alpha)^a_{ev',ev} = (I_R^\alpha)^a_{ev',ev} - (I_L^\alpha)^a_{ev',ev} \tag{1.12b}$$

$$\text{DCP}_\text{I}\ \text{ROA} \quad (\Delta I_I)^a_{ev',ev} = \left(I^R_R\right)^a_{ev',ev} - \left(I^L_L\right)^a_{ev',ev} \tag{1.12c}$$

$$\text{DCP}_\text{II}\ \text{ROA} \quad (\Delta I_{II})^a_{ev',ev} = \left(I^R_L\right)^a_{ev',ev} - \left(I^L_R\right)^a_{ev',ev} \tag{1.12d}$$

The definition of the corresponding total Raman intensity is given as the sum, not the average, of the intensities for right and left circularly polarized radiation.

$$\text{ICP-Raman} \quad (I_\alpha)^a_{ev',ev} = \left(I^R_\alpha\right)^a_{ev',ev} + \left(I^L_\alpha\right)^a_{ev',ev} \tag{1.13a}$$

$$\text{SCP-Raman} \quad (I^\alpha)^a_{ev',ev} = \left(I^\alpha_R\right)^a_{ev',ev} + \left(I^\alpha_L\right)^a_{ev',ev} \tag{1.13b}$$

$$\text{DCP}_\text{I}\text{-Raman} \quad (I_I)^a_{ev',ev} = \left(I^R_R\right)^a_{ev',ev} + \left(I^L_L\right)^a_{ev',ev} \tag{1.13c}$$

$$\text{DCP}_\text{II}\text{-Raman} \quad (I_{II})^a_{ev',ev} = \left(I^R_L\right)^a_{ev',ev} + \left(I^L_R\right)^a_{ev',ev} \tag{1.13d}$$

The intensity of Raman scattering per unit solid angle $\Omega$ collected from a cone of angle $\theta$ and an illumination volume $V$ of sample varies linearly with the incident laser intensity $I_0$ and the molar concentration $C$. Hence, an effective molecular $\text{DCP}_\text{I}$ Raman differential scattering cross-section $[\mathrm{d}\sigma_\text{I}(\theta)/\mathrm{d}\Omega]^a_{ev',ev}$ can be defined by the expression

$$(I_\text{I})^a_{ev',ev} = I_0 NCV[\mathrm{d}\sigma_\text{I}(\theta)/\mathrm{d}\Omega]^a_{ev',ev} \tag{1.14}$$

where $N$ is Avagadro's number. In an analogous manner, the $\text{DCP}_\text{I}$ ROA molecular cross-section $[\Delta\,\mathrm{d}\sigma_\text{I}(\theta)/\mathrm{d}\Omega]^a_{ev',ev}$ can be defined as:

$$[\Delta\,\mathrm{d}\sigma_\text{I}(\theta)/\mathrm{d}\Omega]^a_{ev',ev} = \frac{1}{I_0 NCV(ee)}(\Delta I_\text{I})^a_{ev',ev} = \frac{1}{I_0 NV(C_M - C_m)}(\Delta I_\text{I})^a_{ev',ev} \tag{1.15}$$

and where $(ee)$, the enantiomeric excess, is defined in Equation (1.9). Using the definitions of the lineshape functions for individual Raman transitions for modes labeled $a$, we can express the measured ROA and Raman spectra as sums over individual transitions multiplied by their lineshape functions as:

$$\Delta I_\text{I}(\nu) = \sum_a (\Delta I_\text{I})^a_{ev',ev} f'_a(\nu) \tag{1.16}$$

$$I_\text{I}(\nu) = \sum_a (I_\text{I})^a_{ev',ev} f'_a(\nu) \tag{1.17}$$

### 1.1.4 Unique Attributes of Vibrational Optical Activity

Vibrational optical activity possesses many unique properties that distinguish it from other forms of spectroscopy. As such it will have an enduring place in the set of available spectroscopic probes of molecular properties. These unique attributes are discussed below.

#### *1.1.4.1 VOA is the Richest Structural Probe of Molecular Chirality*

Chirality is arguably one of the most subtle and important properties of our world of three spatial dimensions. Similarly, molecular chirality is one of the most subtle and important characteristics of molecular structure. Of all the available spectroscopic probes of molecular chirality, such as optical

rotation and electronic circular dichroism, VOA is by far the richest in structural detail. The IR and VCD spectra, or Raman and ROA spectra, of a chiral molecule sample contain sufficient stereochemical detail to be consistent with only a single absolute configuration and a unique solution-state conformation, or distribution of conformations, of the molecule. In addition, the magnitude of a VOA spectrum relative to its parent IR or Raman spectrum is proportional to the enantiomeric excess of the sample.

#### *1.1.4.2 VOA is the Most Structurally Sensitive Form of Vibrational Spectroscopy*

VCD and ROA spectra add a new dimension of stereo-sensitivity to their parent IR and Raman spectra, which are already the most structurally rich forms of solution-state optical spectroscopy. VOA spectra possess a hypersensitivity to the three-dimensional structures of chiral molecules that surpasses ordinary IR and Raman spectroscopy. This is most evident in the VOA spectra of complex biological molecules, such as peptides, proteins, carbohydrates, and nucleic acids, in addition to biological assemblies such as membranes, protein fibrils, viruses, and bacteria. In many cases, VOA spectra exhibit distinct differences in the conformations of biological molecules that are only apparent in the IR and Raman spectra as minor, non-specific changes in frequency or bandshape.

#### *1.1.4.3 VOA Can be Used to Determine Unambiguously the Absolute Configuration of a Chiral Molecule*

VOA measurements compared with the results of quantum chemistry calculations of VOA spectra can determine the absolute configuration of a chiral molecule from a solution or liquid state measurement without reference to any prior determination of absolute configuration, modification of the molecule, or reference to a chirality rule or approximate model. Samples need not be enantiomerically pure and minor amounts of impurities can be tolerated. By contrast, the determination of absolute configuration using X-ray crystallography requires single crystals of the sample molecules in enantiomerically pure form. VOA provides either a supplemental check or a viable alternative to X-ray crystallography for the determination of the absolute configuration of chiral molecules. As a bonus, the solution- or liquid-state conformational state of the molecule is also specified when the absolute conformation is determined.

#### *1.1.4.4 VOA Spectra Can be Used to Determine the Solution-State Conformer Populations*

Vibrational spectroscopy, as well as electronic spectroscopy, is sensitive to superpositions of conformer populations as conformers interconvert on a time scale slower than vibrational frequencies. VOA spectra of samples containing more than one contributing conformer can be simulated by calculating the VOA of each contributing conformer and combining the conformer spectra with a population distribution of the conformers. When a close match between measured and theoretical simulated VOA and parent IR or Raman spectra is achieved, the solution-state population of conformers used in the simulation is a close representation of the actual solution-state conformer distribution. By contrast, NMR spectra represent only averages of conformer populations interconverting faster than the microsecond timescale. As a result, for such conformers, VOA is currently the only spectroscopic method capable of determining the major solution-state conformers of chiral molecules with more than one contributing conformer.

#### *1.1.4.5 VOA Can be Used to Determine the ee of Multiple Chiral Species of Changing Absolute and Relative Concentration*

VCD and ROA are the only forms of optical activity with true simultaneity of spectral measurement at multiple frequencies. For VCD this is achieved with Fourier transform spectroscopy and ROA uses multi-channel array detectors called charge-coupled device (CCD) detectors. All other forms of optical activity are either single-frequency measurements or scanned multi-frequency measurements.

The structural richness of IR or Raman spectra permits the determination of the concentration of multiple species present in solution as a function of time for a single non-repeating kinetic process. The corresponding VCD and ROA spectra depend on both the concentrations and the *ee* values of the multiple chiral species present. The *ee* of multiple species as a function of time can be extracted from VOA spectra by first eliminating their dependence on the concentration of the species present. As a result, VOA has the potential to be used as a unique *in situ* monitor of species concentration and *ee* for reactions of chiral molecules.

While VOA has many unique advantages and capabilities, as highlighted above, most problems of molecular structure are best approached by a combination of techniques. In addition, VOA cannot presently be used in all cases, such as low concentration or rapid timescales, where other methods, such as electronic circular dichroism or femtosecond spectroscopy, have been successfully used. Nevertheless, VOA does have a unique place among the many powerful spectroscopic methods available for molecular structure determination in diverse environments. It should be mentioned that recently VCD has been measured with sub-picosecond laser pulses raising the prospect that the limitation of VCD measurement with rapid time evolution may be overcome in the near future.

## 1.2 Origin and Discovery of Vibrational Optical Activity

The emergence of VOA in the early 1970s was preceded by many earlier efforts to uncover the effects of vibrational transitions in optical activity spectra, primarily optical rotation measurements in the near-infrared and infrared regions. Tracing the origins and subsequent development of ROA and VCD can only be done at a relatively superficial level. What follows in this and subsequent sections is an attempt to capture the highlights of this story, but leaving out many closely related developments that cannot be included by virtue of limited space. A more complete description of the history and development of VOA requires its own dedicated treatment in order to arrive at a more thorough account of all the key events.

### 1.2.1 Early Attempts to Measure VOA

The discovery of optical activity in electronic transitions pre-dates the discovery of vibrational optical by more than a century. The measurement of optical rotation (OR) dates back to early nineteenth century (Arago, 1811) when the rotation of the plane of polarized light passing through quartz was first measured. Subsequently, the same phenomenon in simple chiral organic liquids was observed for the first time (Biot, 1815). The first measurements of circular dichroism (CD), the differential absorption of opposite circular polarization states, were not achieved until much later (Haidinger, 1847) and were made in the amethyst form of quartz. CD in liquids was not measured until nearly 50 years later (Cotton, 1895) for solutions of chiral tartrate metal complexes. For those interested in further details of the origins of natural optical activity, several excellent reviews have been written of the history and development of optical activity and the origins of circular polarization of radiation and molecular chirality (Lowry, 1935; Mason, 1973; Barron, 2004). As will be shown in detail in Chapter 3, OR and CD are closely related phenomena. The presence of OR at any wavelength in the spectrum of a sample requires the presence of CD at the same or a different region of the spectrum, and vice versa. Because OR is a dispersive phenomena related to the index of refraction, it appears virtually throughout the spectrum at some level. As such, it is always accessible for measurement, whereas CD is restricted to those regions of the spectrum where absorption bands occur.

The search for vibrational optical activity followed a path similar to that of electronic optical activity just discussed. Early attempts to measure vibrational optical activity consisted of measurements of OR extending to longer wavelengths towards the infrared spectral region. The earliest such measurements (Lowry, 1935) yielded no indications that new sources of CD might lie in the vibrational

region of the spectrum. Anomalous OR in $\alpha$-quartz (Gutowsky, 1951) was reported for the infrared region, but this was challenged and not contested (West, 1954), and was attributed to an instrumental artifact. Similarly, reports of anomalies in the OR of chiral organic liquids were published (Hediger and Gunthard, 1954), but later these observations were also concluded to be instrumental artifacts (Wyss and Gunthard, 1966).

The earliest indication of VCD was the measurement of OR in the near-infrared (near-IR) region (Katzin, 1964) where the monotonic behavior of the OR curve with wavelength (also known as ORD) in $\alpha$-quartz, indicated a source of CD further into the IR region. Similar conclusions were reached a few years later (Chirgadze *et al*., 1971) regarding samples of chiral polymers. These two reports refer only to indirect measurements of VOA using OR, and not of the VOA in the region of the originating vibrational transition, called a Cotton effect. Beyond this point in the history of VOA, no further OR measurements, either in the near-IR or the IR region, were reported until recently, as mentioned above and discussed further in Chapter 3 (Lombardi and Nafie, 2009). This absence of VORD occurred because instrumental artifacts are difficult to control for very small OR measurements, and because OR curves are difficult to translate into quantities of direct quantum mechanical significance.

### 1.2.2 Theoretical Predictions of VCD

The discovery of CD in vibrational transitions from isolated molecules was guided by early theoretical studies. These efforts described VCD intensities through a blend of simple models of CD with those for vibrational absorption intensities. Two theoretical predictions were particularly important in that they predicted VCD intensities that appeared to be within the range of measurable magnitude. The need to resort directly to simple models of VCD, rather than full quantum formulations of VCD stemmed from the fact, as we shall see in detail in Chapter 4, that a complete theoretical description of VCD is not possible within the Born–Oppenheimer approximation. This failure occurs because the electronic contribution to the magnetic-dipole transition moment vanishes for a vibrational transition taking place within a single electronic state of the molecule. This failure yielded a physical inconsistency, as the unscreened nuclear contribution to VCD intensity proved to be no problem whatsoever. Thus, the theory of VCD appeared to possess an internal enigma, and it was not at all clear prior to its experimental discovery whether VCD would be an observable phenomenon. As a result, the publication of simple model calculations was vital for the advancement of the field beyond the level of intellectual speculation. It was not until the early 1980s that the theory of VCD was understood in depth for the first time.

The first model formulation of VCD that could be applied to simple chiral molecules (Holzwarth and Chabay, 1972) was based on the coupled oscillator model of electronic CD (See Appendix A for theoretical description). The problem of the vanishing electronic contribution to the magnetic-dipole transition moment in the Born–Oppenheimer approximation was avoided by developing an expression for VCD based on a pair of chirally-disposed electric-dipole transition moments. If two coupled electric-dipole vibrational transition moments in a molecule are separated in space and twisted with respect to one another, their vibrational motion supports both VA and VCD. The pair of transition moments can be thought of as a coupled-dimer pair of vibrations and their transitions as the action of a coupled-oscillator pair of transitions. This model of CD is known as the coupled oscillator (CO) or exciton coupling model and is described theoretically in Appendix A. The two coupled oscillators result in two vibrational transitions that are slightly separated in frequency and have vibrational motions that are in- and out-of-phase leading to a characteristic VCD couplet that is either positive–negative from high to low frequency in the spectrum or the reverse depending on the twist angle of the two oscillators. In the mirror-image (enantiomer) of the chiral molecule, the structure of the pair of oscillators is identical but the twist angle, and hence the sense of the VCD couplet, is the opposite. The predicted ratio of VCD to VA intensities for typical values of the electric-dipole

transition moments of the dimer pair were reported to be in the range of from $10^{-4}$ to $10^{-5}$, which was just within reach of infrared CD instrumentation available at the time.

A year later, a paper was published (Schellman, 1973) that gave further impetus to the search for VCD spectra. In this paper, VA and VCD intensities were modeled by assigning a charge to each nucleus that represents the nuclear charge minus a fixed electronic screening of the nuclear charge. The motion of these fixed partial charges located at the nuclei of a chiral molecule provided sufficient physics for the determination of the electric- and magnetic-dipole transition moments, and hence VA and VCD intensities, for any vibrational mode in the molecule. The problem of the vanishing contribution of the electrons to the magnetic-dipole transition moment was avoided by transferring that contribution, as static quantities, to the nuclear contribution where no such problem was present. Here again, predicted intensities were in the range of from $10^{-4}$ to $10^{-5}$ for the ratio of VCD to VA for particular transitions. This method of calculating VCD intensities, although somewhat crude, is important because of its generality and absence of assumptions on the nature of the chiral molecule or its vibrational modes. The model subsequently became known as the fixed partial charge (FPC) model remains important today for its conceptual significance. A brief theoretical description of the FPC model is given in Appendix A.

### 1.2.3 Theoretical Predictions of ROA

As with VCD, the discovery of ROA was preceded by theoretical prediction. In this case, a single paper (Barron and Buckingham, 1971) established the theoretical foundation for ROA, both experimentally and theoretically. For ROA, no fundamental enigma is present at the level of the Born–Oppenheimer approximation, and hence there was no impediment to writing down a complete and internally self-consistent theoretical formation. This paper was preceded by a description (Atkins and Barron, 1969) of the Rayleigh scattering of left and right circularly polarized light by chiral molecules. These two papers, taken together, established a completely new form of natural optical activity, namely optical activity in light scattering, which became the theoretical basis for both Rayleigh and Raman optical activity.

The experimental focus of the first ROA paper was a form of ROA that today is known as incident circular polarization (ICP) ROA, defined above in Figure 1.2 and Equation (1.12a), although the SCP form of ROA was also described by means of a quantity termed the degree of circular polarization of the scattered beam. The scattering geometry assumed for ROA measurements was the classical right-angle scattering that was predominant at the time. The ratio of the intensity of ROA to Raman was predicted to be in the range of from $10^{-3}$ to $10^{-4}$, although model calculations were not carried out until after ROA was discovered experimentally. These estimates, as in the case of VCD, were sufficiently encouraging, relative to the sensitivity of existing experimental Raman instrumentation, that several research groups undertook the attempt to measure ROA for the first time.

### 1.2.4 Discovery and Confirmation of ROA

The discovery of the first genuine ROA spectra was reported in 1973, a year before the discovery of VCD was published. Three papers were published in that year from the laboratory of A.D. Buckingham at the University of Cambridge, which were co-authored with postdoctoral associate Laurence D. Barron and graduate student M.P. Bogaard (Barron *et al*., 1973a; Barron *et al*., 1973b; Barron *et al*., 1973c). One of the molecules exhibiting ROA was $\alpha$-phenylethylamine in the spectral region of low frequency vibrational modes between roughly 250 and 400 $cm^{-1}$. This first ROA spectrum is reproduced in Figure 1.3 (left) for both enantiomers of $\alpha$-phenylethylamine (Barron *et al*., 1973a). The reported ROA spectra from all three of these papers remained unconfirmed

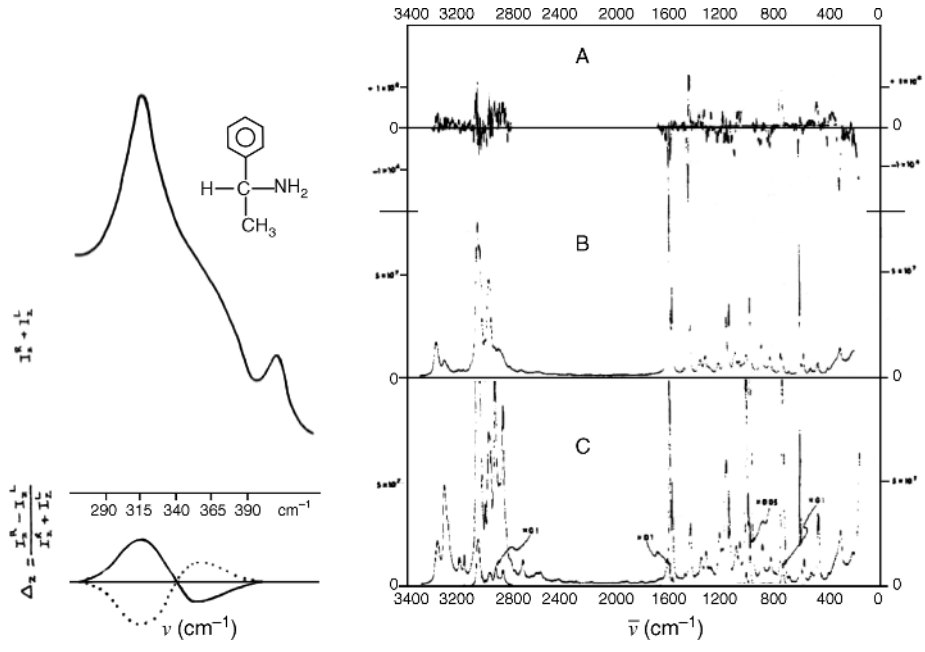


***Figure 1.3*** *Discovery (left) and confirmation (right A) of the ROA spectrum of a neat liquid sample of (+)-α-phenylethylamine with the depolarized Raman spectra (left, and right B) and the polarized Raman spectrum C. Reproduced with permission from the American Chemical Society (Left: Barron et al., 1973c; Right: Hug et al., 1975)*

until 1975 when Werner Hug, working the laboratory of James Scherer at the University of California, confirmed the ROA measurement of neat $\alpha$-pinene and $\alpha$-phenylethylamine (Hug *et al*., 1975). This work also extended the spectral range of measurement to include fundamental normal modes from approximately 200 to 3400 $cm^{-1}$. This confirmation spectrum is shown in Figure 1.3 (right).

It should be noted that in 1972 a research group from the University of Toronto (Bosnick *et al*., 1972) and then in early 1973 from the University of Toledo (Diem *et al*., 1973) published papers reporting ROA (termed Raman circular dichroism in the first case and circularly differential Raman in the second) from simple chiral liquids. In both cases, samples of mirror-image pairs of molecules gave equal and oppositely signed ROA spectra, although all the bands in the ROA spectra of each enantiomer were the same sign. Both of these ROA spectra, measured in polarization perpendicular to the scattering plane, where polarized Raman scattering is present, were eventually shown to be the result of instrumental polarization artifacts sensitive to the optical alignment and possibly the optical rotation of the chiral sample molecules. The genuine ROA spectra reported from Cambridge were measured in parallel polarization as depolarized Raman scattering, and were approximately an order of magnitude smaller, with the signs of the ROA varying across the spectrum between positive and negative values for different vibrational modes of the same molecule. These early erroneous reports threw an air of caution into the search for the first genuine VCD spectra, which was underway at the same time that the discovery and verification of ROA was taking place.

### 1.2.5 Discovery and Confirmation of VCD

The first measurement of VCD for a vibrational mode of an individual molecule was published in 1974 from the laboratory of George Holzwarth at the University of Chicago (Holzwarth *et al*., 1974). The sample was 2,2,2-trifluoromethyl-1-phenylethanol as a neat liquid. This paper was co-authored by postdoctoral associate E.C. Hsu with collaborators Albert Moscowitz and John Overend of the University of Minnesota, who provided theoretical support, and Harry Mosher from Stanford University, who provided the sample. The vibrational mode was the lone methine C–H stretching mode of the hydrogen on the asymmetric carbon center of this chiral molecule. This first published spectrum of VCD is reproduced in Figure 1.4 (left). It consists of the VCD spectra of the (+)-enantiomer, the (–)-enantiomer and the racemic mixture. It is clear from this figure that this first VCD spectrum is just barely discernable above the noise of the VCD spectrometer. Because of the difficulties encountered with the discovery of ROA, discussed above, this result stood for more than a year as an unconfirmed report until this first spectrum was measured and confirmed independently by a different research group using an IR-CD instrument of a different design.

The confirmation of Holzwarth's measurement was published from the laboratory of Philip J. Stephens at the University of Southern California in 1975 and was co-authored by postdoctoral associates Laurence A. Nafie and Jack Cheng (Nafie *et al*., 1975). As with ROA, the original measurement was not only confirmed but was improved and extended to other vibrational modes. The VCD spectrum of 2,2,2-trifluoromethyl-1-phenylethanol confirming the discovery of VCD is presented in Figure 1.4 (right).

In addition to the VCD spectrum in the C–H stretching mode, strong VCD spectra were also recorded in the free and hydrogen bonded OH stretching region. In 1976, the first full paper on VCD was published by Nafie, Keiderling, and Stephens, extending the measurement of VCD to dozens of otherwise non-exceptional chiral molecules in the hydrogen stretching region (Nafie *et al*., 1976). This paper showed that instrumentation could be constructed for the

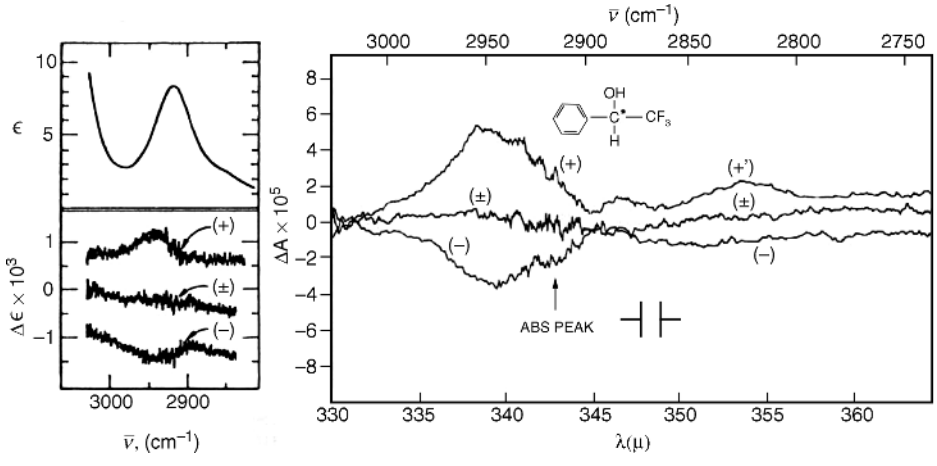


***Figure 1.4*** *Discovery (left) and confirmation (right) of VCD spectra from individual molecules for a sample of neat 2,2,2-trifluoro-1-phenylethanol. Reproduced with permission from the American Chemical Society (Left: Holzwarth et al., 1974; Right: Nafie et al., 1975)*

routine measurement of the VCD spectra of ordinary chiral molecules, including metal complexes and polymers.

## 1.3 VCD Instrumentation Development

Instrumentation for the measurement of VCD spectra has undergone several stages of significant advancement, which we briefly discuss here. More complete descriptions of these advances will be provided in Chapter 6 where VCD instrumentation is considered in detail.

### 1.3.1 First VCD Measurements – Dispersive, Hydrogen-Stretching Region

The first instruments constructed for measuring VCD spectra were dispersive scanning instruments extended from operation in the visible and near-IR regions (Osborne *et al*., 1973) to cover the wavelength regions of the hydrogen-stretching and mid-IR vibrational frequencies. The hydrogen-stretching region extends from 4000 to 2000 $cm^{-1}$, or 2.5 to 5.0 microns (μm). It consists primarily of fundamentals of O–H, N–H, and C–H stretching modes, as well as their deuterium analogs, O–D, N–D, and C–D stretching modes. The higher-frequency region from 4000 to 14 000 $cm^{-1}$ is widely regarded as the near-IR region populated by overtone and combination bands of fundamental vibrational modes, as well as low-lying electronic states of some metal complexes. The region from 2000 $cm^{-1}$ to approximately 400 $cm^{-1}$ is usually called the mid-IR region.

The first VCD measurements, which took place in the hydrogen-stretching region, were made possible by several important technological advances that permitted measurements of absorbance intensities in the IR to the level of $10^{-5}$ absorbance units. These advances were: (i) liquid-nitrogen cooled semiconductor detectors with low noise and response times in the region of 1 μs, (ii) infrared photoelastic modulators (PEMs) with high modulation frequencies and large optical apertures of IR-transparent materials, and (iii) solid-state lock-in amplifiers with high-stability, low-noise and high gain. The components used for the first VCD measurement at the University of Chicago were a Nernst glower source, a Ge PEM, and an InSb photovoltaic detector, whereas the group at the University of Southern California (USC) employed a quartz-halogen lamp, two ZnSe PEMs and an InSb detector. The InSb detector has a low-frequency cut-off near 2000 $cm^{-1}$ and responds electrically to individual photon strikes as opposed to standard IR detectors, which depend on the slower thermal diffusion process. The fast response of the semiconductor detectors was critical for following the modulation frequency of the PEMs, which are in the frequency region of tens of kilohertz. The two PEMs used at USC represented a significant optical advance known as polarization scrambling (Cheng *et al*., 1975), in which the second PEM is operated at a slightly different PEM frequency from the first PEM and at a specific optical retardation to eliminate large sources of VCD artifacts that had plagued measurement attempts with a single PEM.

### 1.3.2 Near-IR VCD Measurements

With capability established for measuring VCD in the hydrogen-stretching region, Keiderling and Stephens carried out the first near-IR VCD measurement of combination bands and overtones (Keiderling and Stephens, 1976). Essentially the same instrumentation employed in the hydrogen-stretching region was used except that an InAs detector, with a cutoff of close to $3000^{-1}$ was substituted for the InSb detector. More than a decade passed before Abbate undertook additional near-IR VCD measurements (Abbate *et al*., 1989) by converting a visible electronic CD spectrometer into near-IR operation to about 6000 $cm^{-1}$. The emphasis of this work is the study of the VCD of second and higher overtones of fundamental CH-stretching vibrational modes.

### 1.3.3 Mid-IR VCD Measurements

The low-frequency limit of VCD observation in the first few years following the discovery of VCD was about 2800 $cm^{-1}$, the low-energy limit of CH stretching vibrations. This limit was extended considerably in 1978 to 1600 $cm^{-1}$ using a PbSnTe detector on the USC dispersive VCD spectrometer (Stephens and Clark, 1979). In 1980, Keiderling, at the University of Illinois, Chicago, extended VCD measurements through much of the mid-IR to approximately 1200 $cm^{-1}$ using an HgCdTe detector (Su *et al*., 1980). Further extension of VCD in the mid-IR did not occur until Fourier transform (FT) VCD spectrometers were developed and optimized by Nafie and co-workers at Syracuse University where vibrational transition to as low of 800 $cm^{-1}$ were measured (see the next section). Following the advent of FT-VCD instrumentation, the low-frequency limit of VCD measurement was extended to 650 $cm^{-1}$ (Devlin and Stephens, 1987) using dispersive instrumentation and a silicon detector with a low frequency cut-off. Attempts to extend this limit to 300 $cm^{-1}$ using a Fourier transform polarization division interferometer were reported (Polavarapu and Deng, 1996) but currently remain uncertain due to the small size of the possible VCD features relative to the noise level.

### 1.3.4 Fourier Transform VCD Instrumentation

The theory of rapid-scan double modulation Fourier transform difference spectroscopy, with application to both circular and linear dichroism, or any other high-frequency modulation of the IR beam, was published in 1979 (Nafie and Diem, 1979). The concept of Fourier transform CD measurement had been pursued and demonstrated in France in the 1960s using step-scan instrumentation in the visible region of the spectrum (Russel *et al*., 1972). The double modulation rapid-scan approach used the idea of inserting a PEM, operating in the tens of kilohertz region, prior to the sample in an FT-IR spectrometer and separating the double-modulated high-frequency VCD interferogram from the much lower frequency ordinary IR interferogram using electronic filters. The output of a lock-in amplifier tuned to the PEM frequency with a sub-millisecond time constant produces a VCD interferogram that can be Fourier transformed and further processed to produce a final VCD spectrum.

Based on this methodology, the first FT-VCD measurements were carried out by Nafie and Vidrine at the headquarters of the Nicolet Instrument Corporation in Madison, Wisconsin, USA, in the summer of 1978 (Nafie *et al*., 1979). These measurements employed an InSb detector and yielded FT-VCD in the medium-IR region for the CH-stretching modes of camphor. Subsequently, at Syracuse University in 1981, FT-VCD measurements were extended to the mid-IR region where VCD spectra of high quality and high spectral resolution were measured from 1600 to 900 $cm^{-1}$ for a variety of chiral organic molecules, thus demonstrating the generality of FT-VCD instrumentation (Lipp *et al*., 1982). The low-frequency limit of these measurements was imposed principally by the cut-off of the type-A HgCdTe (MCT) detector with a low-frequency limit of detection of approximately 800 $cm^{-1}$. This advance not only ushered in a new era of VCD measurements in terms of simultaneous quality, resolution and spectral range of VCD measurement, but it opened the mid-IR region to routine measurement of VCD and considerably eased the task of constructing a VCD spectrometer. One could now begin construction of a VCD spectrometer starting from a sophisticated computer-controlled FT-IR spectrometer. Only the VCD accessory bench and auxiliary electronics needed to be assembled. This brought VCD instrumentation within the reach of manufacturers of FT-IR spectrometers and ultimately led to the commercialization of VCD spectrometers in the 1990s.

### 1.3.5 Commercially Available VCD Instrumentation

The commercialization of instrumentation for VCD measurements took place gradually. Both BioRad (Digilab) and Nicolet (now Thermo Nicolet) helped interested customers equip their FT-IR spectrometers with VCD accessory benches in the mid- to late 1980s, but neither company actively advertised

VCD in their product literature. Throughout the early 1990s, both Nicolet and BioRad were helping VCD researchers (Nicolet with Nafie at Syracuse University and BioRad with Keiderling at the University of Illinois, Chicago) in various ways and were learning from them how to best equip an FT-IR spectrometer for VCD operation. With the advent of step-scan FT-IR instrumentation in the mid-1990s, interest in the possibility of commercially available VCD increased further, and Bruker started working with Nafie at Syracuse University to develop a commercial VCD accessory.

A major breakthrough in commercial VCD instrumentation occurred when Rina Dukor, alongwith Nafie, formed BioTools Inc., and convinced Henry Buijs and Garry Vail at Bomem Inc., an FT-IR manufacturer in Quebec City, Canada, to team with BioTools to build a dedicated FT-VCD spectrometer optimized with hardware and software for VCD measurement. In 1997, Bomem and BioTools, in a joint venture, introduced the Chiral*IR* FT-VCD spectrometer to the market place as the first stand-alone, fully-dedicated instrument for VCD operation. This instrument revolutionized the field of VCD. For the first time, one could watch VCD spectra being collected and improved second-by-second with each FT-scan, as the various steps of phase correction of interferograms, division of VCD transmission by IR transmission spectra, and intensity calibration were automatically incorporated into the spectral collection and output displays.

Following this advance, other FT-IR manufactures, such as Nicolet, BioRad (now Varian), and Bruker offered improved VCD accessory benches with dedicated software for VCD measurements. However, the Bomem–BioTools VCD instrument (now assembled solely by BioTools) remained the only single platform VCD spectrometer with factory pre-aligned optics available commercially. More recently, Jasco has commercialized a single-platform VCD spectrometer in Japan. In 2009 BioTools offered a second-generation FT-VCD spectrometer called the Chiral*IR-2X* in which all electronics processing is reduced to a single PC card in the VCD computer, and up to three interferograms can be collected simultaneously, one for the normal IR spectrum and two for the VCD and the VCD baseline, the latter two of which are dynamically subtracted with each interferogram scan.

Over the past several years the number of research groups involved in measuring or calculating VCD has increased from approximately four to well over 50, more than an order of magnitude, with the level of interest and activity increasing each year.

## 1.4 ROA Instrumentation Development

The construction of an ROA instrument that is relatively free of optical artifacts is much more difficult to achieve than the corresponding instrumentation for VCD. As a result, prior to the development of commercially available ROA instrumentation, the prevalence of ROA instrumentation world-wide was limited, except for brief efforts, to essentially three research groups, namely those of Laurence Barron in Glasgow, UK, Werner Hug in Fribourg Switzerland, and Laurence Nafie in Syracuse, New York, USA, and where only the instruments at Glasgow and Syracuse have maintained activity over the 30 years since the discovery of ROA. In this section, the historical development of the major advances in ROA instrumentation is briefly described, with more technical details provided in Chapter 7 on ROA instrumentation.

### 1.4.1 First ROA Measurements – Single Channel ICP-ROA

The first ROA measurements were carried out with dispersive scanning monochromators equipped with single-channel photomultiplier tube detectors and photo-counting electronics. The optical layout was right-angle scattering and the polarization modulation scheme was depolarized ICP-ROA. In particular, the incident laser radiation was square-wave modulated between right and left circular polarization states and the scattered light was passed through a linear polarizer that was set to be parallel to the plane of scattering, thus producing depolarized Raman scattering intensities

and eliminating polarized Raman scattering. The earliest measurements used either the 448 or the 514 nm lines of an argon ion laser. An advance using this basic instrumentation included the first measurements of anti-Stokes ROA in Glasgow, which confirmed the theoretical prediction of the signs and intensities for this type of ROA (Barron, 1976).

### 1.4.2 Multi-Channel ROA Measurements

Multi-channel ICP-ROA measurements were reported from the laboratory of Werner Hug at the University of Fribourg in 1979 (Hug and Surbeck, 1979) and shortly thereafter from the laboratory of Martin Moskovits at the University of Toronto (Brocki *et al.*, 1980). Multi-channel detection overcomes one of the most serious drawbacks of ROA measurement, namely the length of time required for the detection of a spectrum with sufficient signal-to-noise ratio. Multi-channel detection reduces the time required by nearly two orders of magnitude, thus dramatically increasing the access of ROA spectra to experimental measurement. The measurements of Hug also featured a dual arm collection scheme that permitted the first reported measurements of ROA in perpendicular polarization (polarized ICP-ROA) where artifacts were reduced by cancellation of artifacts of opposite sign in the two collection arms.

### 1.4.3 Backscattering ROA Measurements

In 1982, Hug reported the design of an ICP-ROA instrument for measurements in backscattering geometry (Hug, 1982). Unfortunately, this instrument, as well as Hug's entire ROA laboratory, was destroyed by a fire in the Chemistry Department at the University of Fribourg. With insufficient funds to reconstruct his laboratory, Hug turned his attention for several years to theoretical calculations of ROA; however, in 1989, with encouragement from Laurence Barron, he collaborated with Barron by providing parts recovered from his 1982 instrument to build a new backscattering ROA spectrometer in Glasgow (Barron *et al.*, 1989). This work included the first measurements of ROA with a charged-coupled device (CCD) detector and revolutionized the measurement of ICP-ROA by reaching unprecedented levels of speed of collection and spectral quality.

### 1.4.4 SCP-ROA Measurements

The theoretical basis for SCP-ROA was established by Barron and Buckingham when they first considering Rayleigh and Raman optical activity in 1971. It was referred to as $P_c$, the degree of circularity of the scattered beam, if linear polarized light was incident on the sample. However, it was regarded more as a theoretical curiosity rather than an ROA intensity that could be readily measured with available technology. The conceptual barrier was that the definition of $P_c$ was couched more in terms of a single property of scattered light, the small degree to which left or right circularly polarized was in excess for the various Raman scattering intensities.

However, in 1988 Nafie reasoned that the entire scattered beam could be thought of as consisting of only left and right circularly polarized contributions. The contributions could be measured separately by using a zeroth-order quarter-wave plate such that one circular component would be converted into vertically-polarized intensity and the other circular component would be horizontally-polarized intensity. The two circular polarization components of the scattered beam could be then be separately measured by using a linear polarizer to select either the right or left circularly polarized component of the scattered radiation. If these two intensities were added, the ordinary polarized or depolarized Raman spectrum would be obtained, and if subtracted, the $P_c$ could be measured, not as a single measurement but as the difference of two Raman spectra, in the same way that ICP-ROA was measured by switching the circular polarization states of the incident light back and forth and measuring the

difference in Raman intensities. To draw attention to this analogy, the measured $P_c$ spectrum was referred to as scattered circular polarization ROA or SCP-ROA (Spencer *et al*., 1988). Subsequently, with the help of Lutz Hecht and Diping Che, this instrument was redesigned and upgraded (Hecht *et al*., 1991) to allow detailed comparisons of ICP-ROA and SCP-ROA of the same sample under the same instrument conditions (Hecht *et al*., 1992).

### 1.4.5 DCP-ROA Measurements

The demonstration of the feasibility of the measurement of ICP and SCP forms of ROA led to the theoretical prediction of two new dual circular polarization forms of ROA (Nafie and Freedman, 1989), designated $DCP_I$-ROA and $DCP_{II}$-ROA and defined in Section 1.1.3. Backscattering $DCP_I$-ROA is a purely depolarized form of ROA, and is the most efficient form of ROA relative to the intensity of the parent Raman spectrum, $DCP_I$-Raman, that can be performed. On the other hand, $DCP_{II}$-ROA is a very weak effect that vanishes in the far-from-resonance (FFR) approximation. The first measurements of $DCP_I$-ROA were published in 1991 and confirmed the theoretical prediction of the effect made two years earlier (Che *et al*., 1991). In general, the sum of $DCP_I$-ROA and $DCP_{II}$-ROA equals $ICP_u$-ROA, that is ICP-ROA measured with no analyzer or polarization discrimination in the scattered beam. In 1994, $DCP_{II}$-ROA was measured for the first time as the difference in between backscattering $ICP_u$-ROA and $DCP_I$-ROA in a series of four molecules with increasing double-bond character, starting from *trans*-pinane, which has no functionality (Yu and Nafie, 1994). The corresponding increase in the intensity of the $DCP_{II}$-ROA spectrum with increasing organic functionality signaled the breakdown of the FFR approximation and the onset of pre-resonance Raman intensity.

### 1.4.6 Commercially Available ROA Instruments

The first, and to date the only, commercially available instrumentation for the measurement of ROA was introduced by BioTools Inc., in 2003. The Chiral*RAMAN* spectrometer is an SCP-ROA spectrometer with laser excitation at 532 nm designed along the lines of an SCP-ROA spectrometer built by Hug at the University of Zurich. The details of the optical design of the Hug instrument were described first (Hug and Hangartner, 1999) and its artifact reduction features were published a few years later (Hug, 2003). Hug's design embodies a number of novel features that make the measurement of ROA routine and more efficient than any ROA or Raman spectrometer previously constructed. The most significant of these is that the right and left circularly polarized scattered radiation are measured simultaneously on the upper and lower halves of the CCD detector, thereby eliminating the effects of laser intensity variations and sample flicker noise in the measured SCP-ROA spectrum. The second novel feature of this instrument is the use of electronically-controlled half-wave plates to eliminate linear polarization components and equalize over time any bias in the instrument for detection of left and right circularly polarized scattered light. The result is an instrument that measures SCP-ROA spectra of high quality in a routine fashion thereby freeing the user to focus on the measurement and interpretation of ROA spectra rather than optimizing and adjusting the performance of the instrument.

## 1.5 Development of VCD Theory and Calculations

Understanding the origin of VCD intensities and developing software for calculating VCD intensities has passed through a number of stages, beginning with simple conceptual models and culminating with the current status of sophisticated quantum calculations that closely simulate experimentally measured spectra. The two conceptual models that emerged from considerations of electronic optical activity in the decades preceding the development of VCD were the coupled oscillator model and the

one-electron model for a charge following a helical path. Not surprisingly, both of these conceptual models can be found in the development of descriptions of VCD intensity.

### 1.5.1 Models of VCD Spectra

Models of VCD spectra were important for the development of this field because, as mentioned above, the complete quantum mechanical description of VCD lies beyond the Born–Oppenheimer approximation. A review of the various models developed for the description of VCD has been published that connects these models to the formal theory of VCD (Freedman and Nafie, 1994). The first theoretical model of VCD intensity was published in two papers by Deutche and Moscowitz for vibrational modes in polymers (Deutsch and Moscowitz, 1968; Deutsche and Moscowitz, 1970). The basic idea was that of moving charges on the nuclei that comprised the structure of the polymer. The mathematical formalism used in these papers was complex and simple expressions were not offered that could be generally applied to other situations.

#### *1.5.1.1 Coupled Oscillator Model*

The first publication of a model of the VCD having wide applicability was on the coupled oscillator model (Holzwarth and Chabay, 1972) (Appendix A). As noted above, VCD was shown to arise from two identical oscillators in a molecule that were separated by a fixed distance and were skewed relative to one another. These two oscillators were assumed to couple such that two new vibrational modes ensued from their coupling. One was the mode where the two oscillators moved in-phase with respect to each other and the other where they moved out-of-phase. The model predicts VCDs of equal magnitude and opposite sign for the two coupled modes. Estimates of the magnitudes of expected VCD intensities were provided that served as an incentive for the experimental search for VCD spectra. This model was failry general but nevertheless was restricted to cases where two near-identical coupled vibrational motions could be found in a molecule.

#### *1.5.1.2 Fixed Partial Charge Model*

The second early model of VCD intensity was the fixed partial charge model of VCD intensity (Schellman, 1973) (Appendix A). The model had its conceptual roots in the papers by Deutche and Moscowitz, but more specifically used theoretically derived estimates of the excess positive or negative fractional charge found on the individual nuclei of a molecule. This model shows that IR and VCD intensities can be calculated for any chiral molecule for which partial charges are assigned to each atomic nucleus and for which the relative displacements of each atom in the normal modes of the molecule are known. Predictions of expected VCD intensities were given for selected vibrational modes in a series methyl pyrrolidones, which were encouraging for the observability of VCD.

#### *1.5.1.3 Localized Molecular Orbital Model*

In 1977 Nafie and Walnut published the first model of VCD that used a quantum mechanical description of the electronic motion (Nafie and Walnut, 1977) (Appendix A). In this approach, the molecular orbitals of the molecule are first localized (LMOs) by one of several available methods, resulting in orbitals with pairs of electrons corresponding to inner shell atomic orbitals, bonding orbitals, and lone pairs. The motion of the centroid (average position) of charge of each LMO is combined with the motion of each nucleus during a normal mode to predict the VA and VCD intensity.

#### *1.5.1.4 Charge Flow Model*

A generalization of the FPC model was published in 1981 by Abbate, Laux, Overend, and Moscowitz (Abbate *et al*., 1981) and a similar version was published soon thereafter (Moskovits and Gohin, 1982). The idea is to permit the fixed charges on the nuclei to vary with nuclear motion rather than to remain

fixed, as in the FPC model, leading to charge fluxes at the nuclei and charge currents between nuclei along connecting bond lines. This flexibility overcame a major limitation to the FPC model but was never implemented to any significant extent. Instead, this model was important conceptually as it presaged the solution to the problem of the Born–Oppenheimer approximation.

#### *1.5.1.5 Ring Current Model*

The ring current (RC) model was first proposed in 1983 by Nafie, Oboodi, and Freedman to explain the anomalously large positive VCD associated with the lone methane ($C_\alpha$–H) stretching mode of all the L-amino acids (Nafie *et al*., 1983; Nafie and Freedman, 1986). All previously proposed empirical models of VCD were conservative in the sense that the sum of the VCD over all coupled modes yielded zero net VCD intensity, and thereby could not explain this excess VCD associated with the $C_\alpha$–H stretching modes of the L-amino acids, and subsequently other such modes. The basic idea of the RC model is that a single oscillator generates a ring of vibrationally induced current that is not accompanied by a corresponding motion of the nuclei. The current in the ring generates its own unshielded oscillating magnetic dipole moment that combines with the electric-dipole moment of the current-generating oscillator, such as a CH bond stretch, to produce large monosignate VCD intensity. After many years of successful application, cases were found that did not conform to the prediction of the RC model (Bursi *et al*., 1990) and its active use was discontinued in favor of *ab initio* calculations of VCD. Further discussion of the ring current and other current models of VCD is given in Appendix A.

Other empirical or molecular orbital models of VCD were proposed over time (Freedman and Nafie, 1994), but only the coupled oscillator model in a more general form has persisted past the development of the rigorous formulation of VCD intensity and its subsequent implementation using modern quantum chemistry methods, as described below.

### 1.5.2 Vibronic Coupling Theory of VCD

As mentioned previously, the Born–Oppenheimer (BO) approximation does not include the dynamical response of the electron density in a molecule to nuclear velocity. This problem was solved exactly for the first time (Nafie and Freedman, 1983) where it was demonstrated that the lowest-order correction to the BO approximation contains the missing vibronic coupling term that gives formally equivalent electronic contributions to VA intensities using either the position or the velocity dipole moment operators. By extension, a formally correct and complete description is thereby obtained for the electronic contribution to the magnetic-dipole moment for a vibrational transition within a single non-degenerate electronic state. Subsequently, it was shown (Nafie, 1983a) that the identified BO correction term could be made imaginary by converting a quantum mechanical momentum operator into a classical momentum coordinate, thus producing a missing correlation between electronic current density in molecules correlated with associated classical nuclear velocities. This theory supplements the normal BO correlation between static electron density and classical nuclear positions. The new adiabatic wavefunction having parametric dependence on both classical nuclear positions and velocities is termed the complete adiabatic (CA) wavefunction. The complete vibronic coupling theory (VCT) by necessity includes a summation over all the excited states (SOS) of the molecule, a fact that temporarily impeded the implementation of the theory of VCD for practical calculations for several more years (Dutler and Rauk, 1989).

### 1.5.3 Magnetic Field Perturbation Formulation of VCD

Two years after the VCT theory was published, a magnetic field perturbation (MFP) formulation of VCD was proposed (Stephens, 1985) based on the VCT theory of VCD published by Nafie. This was followed a year later by the implementation of the MFP theory for two simple rigid molecules that were

chiral by deuterium substitution (Lowe *et al*., 1986a; Lowe *et al*., 1986b). The results were encouraging and represented the first VCD spectra calculated from first principles, using *ab initio* quantum mechanical algorithms, without underlying approximations in the theoretical expression used. This represented a major advance to the field of VCD. In the MFP formulation of VCD, it was shown that the explicit non-Born–Oppenheimer sum over electronic excited states in VCT theory could be circumvented by replacing the summation with the algebraically equivalent perturbation of the electronic wave function with an applied magnetic field, even though a magnetic field is not present during a VCD measurement. This step also creates an imaginary component to the electronic wavefunction, which supports the magnetic field generated electronic current density. The MFP formalism was independently developed in the Ph.D. thesis of Galwas at the University of Cambridge under the supervision of Buckingham (Galwas, 1983). This work was subsequently published but calculated VCD intensities were not reported (Buckingham *et al*., 1987).

The SOS and MFP formulations of the VCT theory of VCD intensity are formally the same, but offer different computation routes to the same result. Both formulations sample the physics of all the excited states defined within the finite basis set used for the quantum chemistry calculations. In the MFP formulations the sampling of the excited electronic states takes place within the solution of coupled perturbed Hartree–Fock (CPHF) equations, whereas in the SOS formulation, the excited states are used directly within the second-order perturbation theory with explicit excited-state energies without perturbing the electronic wavefunction in a self-consistent way. In 1989 the SOS formulation of VCT was first implemented for VCD calculations (Dutler and Rauk, 1989).

### 1.5.4 Nuclear Velocity Perturbation Formulation of VCD

In 1992 the third formulation of VCD amenable for use with *ab initio* quantum chemistry programs was published (Nafie, 1992). In the nuclear velocity perturbation (NVP) formulation of VCT theory, the non-BO correction term is parameterized using the classical momenta of the nuclei and is used as an energy perturbation to carry out CPHF theory of the electronic wavefunction. Nuclear velocity dependence of the electronic wavefunction was included by the use of an exponential gauge factor on the atomic orbitals, similar to the gauge factors used to describe so-called London orbitals (London, 1937) or gauge-invariant atomic orbitals (GIAOs) (Ditchfield, 1974). GIAOs are currently used in the calculation of magnetic properties of molecules, where, in the absence of such orbitals, the choice of origin of the magnetic moment operator leads to undesired variation, origin dependence, in the calculated results. The NVP gauge factor carries an explicit dependence of the nuclear velocity of the basis-function orbitals on which the orbitals are centered. As the NVP formulation of VCD is a CPHF approach to VCT theory, it represents an origin-independent alternative to avoid the explicit SOS states of VCT theory. To date the NVP formulation of VCD has not yet been implemented. In the NVP paper of Nafie, it was also demonstrated for the first time that GIAOs in the MFP formation of VCD also produce an origin-independent formulation of VCD intensities. In 1993, the first calculations of VCD using London orbitals were published (Bak *et al*., 1993).

### 1.5.5 *Ab Initio* Calculations of VCD Spectra

Since the first *ab initio* calculations of VCD reported in 1985, a number of significant advances have been made, mostly pioneered by Philip Stephens in collaboration with Michael Frisch at Gaussian Inc. These include overcoming the problem of origin dependence by implementing a distributed origin treatment (Jalkanen and Stephens, 1988) and then implementing GIAOs, testing of basis sets for relative accuracy, testing post-Hartree–Fock programs, such as second order Moller–Plesset (MP2) (Stephens *et al*., 1994) and implementing density functional theory (DFT) and exploring available functionals (Devlin *et al*., 1996). The result of this work is a minimal recommendation for the

calculation of VCD intensities as a GIAO basis set at the level of 6-31G(d) or higher and DFT with hybrid functionals such as B3LYP or B3PW94. These minimal options for VCD calculations are available in several quantum chemistry programs.

### 1.5.6 Commercially Available Software for VCD Calculations

With the breakthroughs in the practical formulation and *ab initio* calculations of VCD intensities, it was not long before quantum chemistry programs included VCD as an option in the menu of available calculated molecular properties. Several quantum chemistry packages have become available for the calculation of VCD intensities. All use the MFP formulation of VCD intensities and offer a variety of choices of basis sets and approaches to intensity calculations. The first of these was the Cambridge Analytical Derivative Program Package (CADPAC, http://www-theor.ch.cam.ac.uk/software/cadpac.html) from the University of Cambridge. The Dalton Program (http://www-theor.ch.cam.ac.uk/software/cadpac.html) from the University of Olso, Norway, and Gaussian 98, 03 and 09 from Gaussian Inc., (www.gaussian.com) in Wallingford, CT, USA soon followed with available VCD subroutines. More recently the ADF programs from the Amsterdam Density Functional (ADF) software packages from Scientific Computing and Modeling (http://www.scm.com/) offer subroutines for calculating VCD and ROA based density function theory (DFT) as opposed to a wider spectrum of quantum chemistry methods. Of these, the Gaussian program package is currently the longest, most established commercially available software for VOA calculations. With the advent of well-maintained software for the calculation of VCD spectra, the power of VCD to elucidate the structure of chiral molecules became significantly enhanced and is now widely available to all who wish to compare the measured and calculated VCD spectra.

## 1.6 Development of ROA Theory and Calculations

The theory of ICP-ROA in the far-from-resonance approximation has been known since 1971, more than a decade before VCD reached an equivalent level of complete theory. Due in part, however, to its greater theoretical complexity as a second-order perturbation phenomena with respect to the interaction of light and matter, ROA theory passed through a long period of intensity models and spectra–structure empirical correlation before the first ROA intensities were calculated using *ab initio* quantum chemistry programs (Polavarapu, 1990). In parallel with this, a more complete elucidation of the theory of ROA ensued where a more general theory was established (Hecht and Nafie, 1991) and limiting cases, such as resonance ROA (Nafie, 1996), were examined. In this section we highlight some of the key developments between the initial statement of the theory and our present day understanding. A complete treatment of ROA theory is given in Chapter 5.

### 1.6.1 Original Theory of ROA

For want of a better term, the original theory of ROA as published by Barron and Buckingham in 1971 described ICP-ROA for right-angle scattering using a theoretical treatment that avoided vibronic detail in the sum over excited electronic states. In this limit, the so-called FFR limit, the resonance response of the molecule is taken to be equivalent for both the incident and scattered radiation, the Raman tensor is symmetric, there are only two Raman invariants and three ROA invariants. This theory was the guiding light of ROA experiments for over a decade before a number of improvements were introduced. The first of these was by Hug where backscattering ICP-ROA was first described (Hug, 1982). Here it was demonstrated that ROA could be measured with several advantages in backscattering compared with the traditional right-angle scattering geometry.

### 1.6.2 Models of ROA Spectra

During the early years of the exploration of ROA, simple models played an important role in understanding the possible origin of significant ROA spectral features. In the absence of *ab initio* calculations, models and empirical correlation between spectra and structure were the only means to understand ROA spectra. Prominent among these models is the perturbed degenerate mode model used to explain bisignate ROA arising from near-degenerate vibrations of locally symmetric groups, such as the degenerate anti-symmetric methyl deformation modes near 1450 $cm^{-1}$. Another important model is the two-group model that predicts bisignate ROA from pairs of coupled locally symmetric polarizability groups. This model is the analog of the degenerate coupled oscillator (DCO) model of VCD, for which many examples have been found experimentally. For ROA, however, few examples of the two-group model of ROA have been identified experimentally, perhaps due to differences in the origins of ROA and VCD intensities. Finally, there is the torsion mode model of ROA intensities that is applicable to low-frequency torsional modes in molecules. These models are extensively described by Barron (2004) in his book on light scattering and optical activity.

### 1.6.3 General Unrestricted Theory of Circular Polarization ROA

In contrast to the original theory, the general unrestricted (GU) theory of ROA describes the full extent of the theory of the various forms and scattering geometries of circular and linear polarization ROA measurements (Nafie and Che, 1994). The forms of circular polarization (CP) ROA have been described from the experimental viewpoint in Section 1.4, but beyond this there are four forms of linear polarization (LP) ROA, yet to be discovered, as described in the next section. Behind these developments lies a rich theory of ROA that has not yet been implemented in commercially available computational software programs. Nevertheless, we describe here what this full theory entails and the key advances in the theory of ROA that have led to its present stage of development.

The first steps toward the full unrestricted theory of ROA were taken by 1985 in a paper describing the asymmetry that arises between Stokes and anti-Stokes ICP-ROA when the symmetry of the Raman and ROA polarizability and optical activity tensors is not assumed (Barron and Escribano, 1985). A closely related symmetry breakdown was also noted between what is now called the ICP and SCP forms of ROA, although the latter form of ROA was called the degree of circular polarization in advance of its experimental discovery and renaming in 1987. Following the experimental discovery of SCP and the theoretical prediction of DCP forms of ROA, the distinct theory of all four forms of CP ROA was described by Hecht and Nafie for all possible scattering angles and typical linear polarization schemes. No assumptions were made that would limit the applicability of the theory (Hecht and Nafie, 1991). The aim of the paper was to compare and clarify the relative advantages and disadvantages of the various ways of measuring ROA. The analysis confirmed that ordinary Raman scattering is described by three Raman invariants, and ten ROA invariants. Experimental schemes can be devised to isolate all three Raman invariants, but only six linearly independent combinations of the ten ROA can be measured.

### 1.6.4 Linear Polarization ROA

While working on the GU theory of ROA, a new form of ROA was discovered in backscattering or forward scattering, known as linear polarization ROA (Hecht and Nafie, 1990). Here linear polarization incident on the sample is scattered with the linear polarization state rotated to the left or the right depending on the sign of the LP ROA. In LP ROA, one uses the imaginary part of the electric-quadrupole ROA tensor and the real part of the magnetic-dipole ROA tensor. It can be shown that the LP ROA tensors are only non-zero in the limit of resonance with one or more particular excited electronic states of the molecule.

### 1.6.5 Theory of Resonance ROA in the SES Limit

The theory of ROA for a molecule in resonance with a single electronic state (SES) is the simplest theoretical expression for ROA scattering (Nafie, 1996). This theory, like the FFR theory, represents a limiting case of the theory of ROA. In this limit, only A-term resonance Raman scattering is present, and it is shown that the resulting ROA borrows all of its sense of chirality from the electronic circular dichroism (ECD) associated with the single resonant electronic state. In fact, it is demonstrated that the ratio of the ECD intensity of this band to the intensity of its parent absorption band, the anisotropy ratio, is equal and opposite in sign to the corresponding ratio of the resonance ROA (RROA) to its parent resonance Raman (RR) scattering intensity for all bands in the spectrum. The opposite sign occurs because of the reverse definition of positive intensity in ROA (right minus left) as debated in the literature (Barron and Vrbancich, 1983; Nafie, 1983b). The direct correlation between SES-RROA and the ECD of the resonant state means that the RROA, in this limit, is monosignate and the same shape as its parent Raman spectrum, only smaller by the anisotropy ratio of the resonant electronic state. Subsequently, the theory was confirmed for a pair of chiral molecules, each with a single electronic state in resonance with the incident laser radiation (Vargek *et al*., 1998). This limit breaks down as resonance with other states becomes important or when the resonance state is vibronically coupled to nearby electronic states. If these other states have ECD of the opposite sign to the resonant state, then the ROA spectrum can begin to have ROA bands of both positive and negative signs. The theory of resonance ROA in the SES limit shows the most primitive association between the occurrence of ROA and the ECD of all the excited electronic states responsible for the Raman polarizability and ROA tensors.

### 1.6.6 Near Resonance Theory of ROA

More recently, a new theoretical limit of ROA has been defined called the near resonance (NR) theory (Nafie *et al*., 2007), which connects the original far-from-resonance (FFR) theory to the SES theory. In the FFR theory, as mentioned above, the Raman tensor is symmetric and there are only two Raman tensor invariants and three ROA tensor invariants. Symmetry in the Raman tensor signifies that the tensor response is equivalent in degree of resonance for the incident and scattered Raman radiation. As resonance is approached, this equivalence of resonance degree breaks down. Once the Raman tensor becomes even slightly non-symmetric, the number of tensor invariants increases from two to three for Raman scattering and three to ten for ROA scattering. In the NR limit differences can been seen theoretically between ICP and SCP ROA and $DCP_{II}$ ROA becomes non-zero. Unlike the FFR limit, the NR limit, although almost as simple in form as the FFR theory, carries the full richness of theoretical structure as the GU theory of Raman and ROA.

### 1.6.7 *Ab Initio* Calculations of ROA Spectra

As mentioned above, the first *ab initio* calculations of ROA were carried out by Polavarapu in 1990. The calculations were carried out at the Hartree–Fock level in the zero-frequency static limit for the incident radiation without correction for origin dependence. Improvement in this methodology was advanced by the use of London (GIAO) orbitals (discussed above for VCD theory) and linear response theory (Bak *et al*., 1994). Using this methodology, calculations of ROA were carried out that were independent of molecular origin and the frequency of the incident radiation was specified rather than set to zero value. More recently, Hug has reported ROA calculations using rarefied basis sets optimized for the calculation of Raman and ROA intensities (Zuber and Hug, 2004). For the Raman and ROA intensities he employed Hartree–Fock linear response theory using London orbitals as implemented in the Dalton Program with a basis set that includes ample diffuse functions but limited polarization functions. The calculation of the optimized geometry, force field, and normal mode displacements

were carried with more traditional basis sets, such as 6-311G**. This dual basis-set approach yielded ROA intensities at the same level of accuracy as an aug-cc-pVDZ basis set, but at a fraction of the cost.

### 1.6.8 Quantum Chemistry Programs for ROA Calculations

As mentioned in the previous section, the Dalton Program has included ROA calculations as an option since 1997. Similarly to their VCD program package, the ROA calculations are implemented at a variety of levels of theory, including self-consistent field (SCF), multiple-configuration SCF (MCSCF), second-order Moller–Plesset (MP2) perturbation theory, coupled-cluster theory, and density functional theory (DFT). The Gaussian program package included ROA calculations starting with Gaussian 03 (Frisch *et al*., 2003) and with further improvements in Gaussian 09 (Frisch, 2009). The ROA subroutines run more slowly than the corresponding VCD subroutines for the same molecule for two reasons. The first is that Raman and ROA intensities place more demanding requirements on the basis set used due to the need to calculate the response of the polarizability and optical activity tensors with the nuclear motion, compared with electric and magnetic dipole moments for IR and VCD. The second reason is that the Gaussian 03 programs for ROA tensor derivatives were executed by finite difference which is very time-consuming, but the Gaussian 09 version has implemented analytic derivatives for the ROA tensor derivatives, which now eliminates this second shortcoming.

## 1.7 Applications of Vibrational Optical Activity

The areas of application of VOA range almost as broadly as those of infrared and Raman spectroscopy with the restriction that the samples be chiral molecules with a measurable amount of enantiomeric excess. There are many ways to classify the applications of VOA. Most commonly, this is done either by the type of sample, the type of measurement, or the type of information obtained. In this section we provide an overview of applications of VOA without considering VCD and ROA separately. In Section 1.8 we will compare and contrast these two pillars of VOA spectroscopy.

### 1.7.1 Biological Applications of VOA

Virtually all biological molecules of significance are chiral. Most of these biological molecules display conformational preferences that are important for their roles as biological agents of structure or dynamics. The structure of complex biological molecules that have well-defined conformations can be determined by X-ray crystallography if the molecule can be isolated, purified, and crystallized. Alternatively, solution-phase determinations at the level of atomic resolution can also be determined by nuclear magnetic resonance (NMR) spectroscopy. Relative to these high-resolution techniques, VOA offers some unique insights and contributions to our understanding of the structure of biological molecules. Firstly, VOA is sensitive to chirality, as is X-ray crystallography, but without the restriction of a single crystalline sample and a single conformational state. Secondly, VOA is measured in solution under a variety of sampling conditions, similar to those of NMR, but NMR is blind to chirality. Further, as mentioned above, VOA is not restricted to the size of the biological molecule for which information can be extracted, as occurs with NMR above a certain molecular weight.

VOA spectra have been measured for amino acids, peptides, proteins, sugars, carbohydrates, oligosaccharides, nucleotides, DNA, RNA, glycoproteins, viruses, and bacteria. In short, all major classes of biological molecules have been investigated. Most studies of biomolecules with VOA have been aimed at correlating spectra with structural changes in the biomolecules on an empirical basis or interpreted in terms of some model of VOA intensity. More recently progress has been made toward the *ab initio* DFT calculation of VCD intensity for oligopeptides with up to as many as 20 residues for

particular secondary structure motifs (Bour and Keiderling, 2005). Parallel with these developments, a sophisticated form of the coupled oscillator model has been used that simultaneously models IR, polarized Raman, depolarized Raman, and VCD for a large number of tripeptides (Schweitzer-Stenner *et al*., 2007). It has been shown that these molecules adopt a regular well-defined solution-state conformation. Similar progress in ROA is possible in principle, but is currently hampered by lower molecular size constraints for carrying out ROA *ab initio* calculations, although some progress in this direction has been made recently (Herrmann and Reiher, 2007).

### 1.7.2 Absolute Configuration Determination

With the availability over the past decade of commercial instrumentation for the routine measurement of VOA spectra, coupled with software packages for the accurate *ab initio* calculation of VOA spectra over almost the same period, a new important area of application has rapidly emerged, namely the determination of the absolute configuration of chiral molecules. Most of this activity has occurred for VCD as both instrumentation for measurement and commercial software for calculation of ROA have been available only since 2004. Nevertheless, everything that has been achieved with VCD in this area can in principle be performed with ROA, albeit not as simply nor as quickly.

Part of the rapid growth in VCD over the past decade, and ROA more recently, has been due to the commercial availability of instrumentation combined with a growing need for proof of absolute configuration in the pharmaceutical industry. More than half of all the new pharmaceutical drugs in discovery, development, and testing are chiral. Before a new pharmaceutical molecule can be presented to a regulatory agency for approval of sale to the general public, the absolute configuration must be known beyond any doubt. The gold standard for the determination of the absolute configuration of a molecule has been single-crystal X-ray diffraction using the Bijovet method. In this method, the absolute stereochemistry of the single crystal sample can be determined from its anomalous X-ray diffraction pattern by using a heavy atom to specify the phase of the diffraction. However, obtaining single crystals of sufficient quality for the determination of absolute configuration can be difficult, and sometimes impossible, to achieve. In the vast majority of such cases, it has been shown that VCD can determine the absolute configuration of such chiral pharmaceutical molecules without ambiguity.

The VCD method of absolute configuration determination is carried out by comparing the experimentally measured solution-phase VCD spectrum with the *ab initio* calculated VCD spectrum (Freedman *et al*., 2003; Stephens and Devlin, 2000). In general, there are several tens of bands to compare in sign and relative magnitude. When a good match is obtained between measured and calculated IR and VCD spectra, the absolute configuration of the physical sample is known because the absolute configuration of the molecular structure used for the theoretically calculated spectrum is known. If the calculated VCD spectrum agrees in relative intensities but with opposite signs, then the wrong enantiomer was chosen for the theoretical calculation, and the problem is easily corrected by multiplying the theoretical spectrum by minus one.

### 1.7.3 Solution-State Conformation Determination

The IR absorption and VCD spectrum of a molecule is sufficiently sensitive that a good match between measured and calculated intensities is not possible unless the correct conformation, or distribution of conformations, of the molecule in solution is first identified. In the case of small to medium sized organic molecules or inorganic complexes, if more than one solution-state conformer is present in significant population, the interchange between conformers occurs on the order of picoseconds, much faster than the NMR timescale. As a result, NMR conformation analysis yields only an average of the conformers present whereas vibrational spectra in general, and VOA in particular, consists of linear superpositions of the contribution of each conformer present. In most cases, as the result of the large

number of vibrational transitions in the spectrum, individual bands can often be found in the measured IR and VCD spectra that are specific to a particular conformer. When a distribution of conformers is identified by *ab initio* calculation and a close match with measured IR and VCD intensities is achieved, the resulting information obtained about the solution-state conformers present is unique. No other technique currently available has the sensitivity to identify solution-state conformer populations of chiral molecules, in addition to the identification of their absolute configuration.

### 1.7.4 Enantiomeric Excess and Reaction Monitoring

One of the simplest applications of any form of optical activity is the measurement of enantiomeric excess (*ee*), also called optical purity, defined earlier in the chapter. A common form of the measurement of optical purity is optical rotation, or specific rotation at a particular wavelength, where the rotation value compared with a known standard gives the *ee* of the sample. Measurement of *ee* was carried out for the first time in 1990 with VCD (Spencer *et al*., 1990) and in 1995 with ROA (Hecht *et al*., 1995). An advantage of using VOA for *ee* measurements is that the molecule is identified by its VOA and parent vibrational spectrum at the same time that its *ee* is measured. This ensures that unknown impurities are not present and that the parent IR or Raman spectrum provides a secondary check on the identity and quantity of sample being measured. In optical rotation, for example, there is no independent check if the concentration of the sample is correct for a known optical pathlength. This is one reason that the temperature must be specified for optical rotation measurements, but no such precaution is normally required for VOA determinations of *ee*.

In VOA, each band in the VOA spectrum represents an independent measure of the *ee* when ratioed to its parent vibrational band or compared with the corresponding VOA intensity of a known standard of the same sample molecule. Owing to the large number of such bands that are unique to each molecular species, and because these bands are well resolved from one another, the possibility exists of simultaneous measurement of the *ee* of more than one molecule at a time. Such a determination is not possible with optical rotation, and is difficult for electronic optical activity because electronic absorption or CD bands are not well resolved or sufficiently distinct from one molecule to another.

Recently it was demonstrated that VCD could be employed to monitor the conversion of one chiral molecule into another by continuous flow-cell sampling where, for a sequence of mid-IR FT-VCD measurements, the mole fractions and the *ee* s of the two molecules were changing as a function of time (Guo *et al*., 2004). In so doing, the ability of VCD to monitor the progress of a reaction of one chiral molecule to another in terms of mole fraction and *ee* of both species was demonstrated. A similar demonstration using near-IR FT-VCD showed that chiral reaction monitoring could be carried out in either the mid-IR and the near-IR as desired with an accuracy of approximately 2% *ee* (Guo *et al*., 2005). FT-VCD reaction monitoring of chiral purity of multiple species is possible not only because of the structural richness of the IR and VCD spectra collected, but because all spectral frequencies are collected simultaneously in Fourier transform spectroscopy, thus eliminating spectral time biasing, which is unavoidable using a scanning spectrometer as required for ECD.

Presently, there are no spectroscopic techniques that combine sensitivity to chirality with traditional forms of kinetics measurements to study the reaction mechanisms of chiral molecules. Moreover, in the industrial sector, there is no process monitoring technique that combines traditional spectroscopic probes, for example near-IR sensors, with chiral sensitivity. VCD offers a unique opportunity to probe the dynamics of reactions of chiral molecules that will become increasingly important as the capabilities of FT-VCD reaction monitoring are realized and implemented.

### 1.7.5 Applications with Solid-Phase Sampling

A new area of VCD application is solid-phase sampling. This has been made possible by the reduction in birefringence artifacts associated with the dual-polarization modulation methodology. Solid-phase

sampling has not been reported for ROA. This may be due to the higher susceptibility of ROA to interference from particle scattering because of the shorter wavelengths in ROA compared with VCD. However, VCD spectra have recently been reported for films of proteins where it was demonstrated that the absence of solvent absorption greatly facilitates the acquisition of spectra and reduces the amount of sample required for measurements (Shanmugam and Polavarapu, 2005). By careful film preparation, VCD spectra almost identical with those of solution can be obtained. Other laboratories have reported VCD in mulls, KBr pellets, and spray dried films, and it has been shown that VCD is very sensitive to the particle-size distribution of the sample and the crystal morphology above the size of the unit cell (Nafie and Dukor, 2007). Solid-phase sampling also permits direct comparison of VCD structure determination with that of X-ray crystallography, however, calculations of VCD for molecular solids has not yet advanced to the state where an accurate VCD spectrum can be calculated for an arbitrary solid. Even without the connection to calculations, structural characterization of solids and solid formulations of pharmaceutical products has become a sensitive new area of application of VCD.

## 1.8 Comparison of Infrared and Raman Vibrational Optical Activity

It is natural to want to compare VCD and ROA. Both are forms of VOA. It is possible to display IR, VCD, Raman, and ROA of the same sample over the same range of vibrational frequencies (Qu *et al*., 1996). When this is done, one finds that VCD and ROA are as different from one another as the parent IR and Raman are from each other, and perhaps even more so because of the added dimension of the sign of each VOA band. It might be suspected that the sign of a VCD band and its ROA companion are related by the common motion of the molecule in that vibrational mode. If there were such a correlation, or anti-correlation given the opposite definition of the sign conventions in VCD and ROA, then the concept of vibrational chirality would have merit. However, no such correlation has been discerned, and one is left to conclude that the sign of a VCD or ROA band has as much to do with the electronic mechanism, dipole moment derivatives with respect to nuclear motion for VCD versus the corresponding polarizability derivatives for ROA, as it does with the chirality of the nuclear motion itself. In this section, a brief comparison of VCD and ROA is provided to give the reader a better appreciation of the relative strengths and weaknesses of these two complementary forms of vibrational optical activity.

### 1.8.1 Frequency Ranges and Structural Sensitivities

ROA was discovered in the low-frequency range below $500\,cm^{-1}$ where, even after almost four decades of development, VCD has yet to be observed. The frontiers of ROA were advanced from low to high frequency, and, even today, ROA intensities in the high-frequency range of hydrogen stretching motions are weak and difficult to measure. By contrast, the frontiers of VCD have been advanced from high to low frequency down to about $600\,cm^{-1}$ but no further. The effective spectral range of VCD is from 600 to $14\,000\,cm^{-1}$ when overtone and combination band transitions are included. By contrast, the range of ROA coverage is from 50 to $4000\,cm^{-1}$, although most ROA spectra are restricted to below $2000\,cm^{-1}$. A great advantage of ROA is the coverage of low-frequency vibrational modes that may be particularly sensitive to the conformation and dynamics of biological molecules. VCD on the other hand has coverage to very high frequencies where near-IR process monitoring applications have the clear potential to become very important.

Both VCD and ROA are sensitive to vibrational coupling in molecules. Their intensities derive from the stereo-specific way in which vibrational motion, including the electronic response, is distributed over the framework of the molecule. There are perceived differences, however, in the sensitivities of VCD and ROA to this motion. Because electric dipole moments can couple through space by a radiative mechanism that differs from through bond mechanical coupling, VCD appears to exhibit through space coupling over distances larger than those seen in ROA. For example, in proteins, VCD

shows large intensities in the amide I region that change dramatically with secondary structure through dipole–dipole coupling of the carbonyl stretching motions, whereas ROA is much more sensitive in the amide III region, that arises from localized hydrogen bending motions near the chiral alpha carbon center of peptides residues, which also vary with secondary structure. These different sensitivities of ROA and VCD make these techniques even more complementary than they might otherwise be. This means that adding an ROA spectrum to a VCD spectrum does more than offer the same information in a different form. Different structural information is emphasized and these two techniques are not redundant in a way that is even more striking than how ordinary IR and Raman are complementary and non-redundant.

### 1.8.2 Instrumental Advantages and Disadvantages

ROA instrumentation is approximately twice as expensive as VCD instrumentation. Some of the added cost derives from the fact that a Raman spectrometer equipped with a multi-element CCD camera is more expensive than an FT-IR spectrometer of similar quality and spectroscopic resolution, and the rest of the cost difference is due to the additional expense associated with the laser. Beyond the cost difference, ROA instruments are more complex than the equivalent VCD instrument. ROA is more difficult to measure than VCD due to the additional sensitivity of ROA to imbalances to circular polarization modulation. The additional sensitivity comes from the variation of a Raman spectrum with different states of relative polarization between the incident and scattered light beams, otherwise known as the depolarization ratio. This ratio is huge relative to ROA intensities, and, as a result, any leakage of the depolarization ratio into an ROA measurement introduces a large instrumental artifact in the spectrum. The effect is most easily noticed in highly polarized bands that have the largest differences between the polarization of the Raman scattering that is parallel versus that perpendicular to the scattering plane. Commercial ROA instrumentation overcomes this sensitivity and other imbalances through a series of additional optical elements and timing circuitry, as described under the development of ROA instrumentation in Section 1.4, and also in Chapter 7.

### 1.8.3 Sampling Methods and Solvents

The most significant difference between sampling for VCD and ROA is the nature of the solvents that are most easily and most commonly used. For VCD, the best solvents are relatively non-polar. If hydrogen is present in the solvent, the deuterated analog is preferred as all hydrogen vibrational bands are shifted to lower frequencies away from solute bands of interest. Polar solvents typically have high absorbances and fewer windows for viewing the VCD spectra of solutes. In the case of water, absorption bands are so broad and intense that VCD spectra can only be obtained for samples in high concentrations using very short pathlengths, usually less the 10 microns (μm). Water, on the other hand, is a weak Raman scatterer, and as a result, aqueous solutions pose no difficulties in the measurement of ROA. This is a significant advantage when studying biological molecules. However, polar solvents have very high Raman scattering intensities that can interfere with the collection of ROA spectra of molecules dissolved in such solvents.

Sampling techniques for VCD and ROA follow closely those associated with their parent IR and Raman spectroscopies. Because the laser beam can be focused to spot sizes measured in microns, sample volumes for ROA can be in the microliter range without loss of light collection efficiency. The volumes of sample required for VCD spectral collection can also be reduced to sub-milliliter amounts by a suitable choice of sample cell that has little if any dead space. In general, it can be concluded that VCD and ROA have differences in sampling methods but neither can be said to be superior to the other.

In the area of sample preparation there is a significant difference between ROA and VCD, particularly for samples of a biological origin. This difference is associated with fluorescence, which

can be very detrimental to the measurement of ROA spectra. In order to measure high quality ROA spectra, samples must be chemically purified to eliminate as many impurities as possible, then filtered with a micron hole size filter, kept free of dust and particulate matter, and if necessary filtered again with activated charcoal. Only distilled, de-ionized water should be used in the preparation of aqueous solutions for ROA measurements. The time invested in sample preparation is more than worth its tradeoff in total measurement time in obtaining a high quality ROA spectrum. No such precautions are needed for solution-phase VCD measurements.

### 1.8.4 Computational Advantages and Disadvantages

Aside from the issue of the non-Born–Oppenheimer contributions necessary for the formulation of VCD intensities, the calculation of VCD spectra is much easier and faster than for ROA spectra. To obtain similar levels of accuracy, lower demands are placed on VCD calculations compared with ROA calculations in terms of basis sets and time required for the completion of runs. ROA requires more sophisticated basis sets with ample diffuse functions to describe the more tenuous behavior off the polarizability of a molecule in its response to incident radiation. Owing to its inherently more complex theoretical expression with higher-order tensors for ROA compared with VCD, and its resulting higher requirements for basis set quality, it appears as though ROA will always be more demanding computationally than VCD.

Neither VCD nor ROA place as many demands on calculations as those required for the calculation of an electronic CD spectrum of comparable quality, as VCD and ROA spectra do not typically depend critically on individual excited electronic states, the properties of which are intrinsically more difficult to calculate than those of the ground state of a molecule. Furthermore, in order to obtain the proper bandshape of an ECD spectrum, the entire vibronic manifold must be calculated, which is similar to calculating the entire VCD spectrum for each band in an ECD spectrum. Based on these considerations, it appears that VCD enjoys a permanent advantage over all other forms of natural optical activity in terms of its structural content and relative ease of accurate calculation. As computers improve and become more powerful in the future, the advantage of VCD and ROA will continue to be present as calculated spectra move closer to their measured counterparts.

## 1.9 Conclusions

In this chapter, a brief outline has been given of the origins, development and current state of the art of VOA. The aim has been to provide an overview of the topics that will be dealt with in more detail in the following chapters. Space does not permit a more detailed description of the history of VOA. By necessity some important developments and contributions have not been included, but could be in a more expanded treatment of this subject. If desired, this chapter could be read in isolation from the rest of the book, not as a comprehensive review, but more of an impressionistic overview of what VOA is, where did it come from, and how did it get to its present state of development. In the following chapters, details are provided in all key areas of VOA for the reader to investigate as desired.

## References

Abbate, S., Laux, L., Overend, J., and Moscowitz, A. (1981) A charge flow model for vibrational rotational strengths. *J. Chem. Phys.*, **75**, 3161–3164.

Abbate, S., Longhi, G., Ricard, L. *et al.* (1989) Vibrational circular dichroism as a criterion for local mode versus normal mode behavior. Near-infrared circular dichroism of some monoterpenes. *J. Am. Chem. Soc.*, **111**, 836–840.

Arago, D.F. (1811) *Mem. de L'Inst.*, **12**, part 1, 93.
Atkins, P.W., and Barron, L.D. (1969) Rayleigh scattering of polarized photons by molecules. *Mol. Phys.*, **16**, 453–466.
Bak, K.L., Jorgensen, P., Helgaker, T. *et al.* (1993) Gauge-origin independent multiconfigurational self-consistent-field theory for vibrational circular dichroism. *J. Chem. Phys.*, **98**, 8873–8887.
Bak, K.L., Jorgensen, P., Helgaker, T., and Ruud, K. (1994) Basis-set convergence and correlation-effects in vibrational circular-dichroism calculations using London atomic orbitals. *Faraday Discuss. R. Soc. Chem.*, **99**, 121–129.
Barron, L.D. (1976) Anti-Stokes Raman optical activity. *Mol. Phys.*, **31**, 1929–1931.
Barron, L.D. (2004) *Molecular Light Scattering and Optical Activity*, 2nd edn, Cambridge University Press, Cambridge.
Barron, L.D., and Buckingham, A.D. (1971) Rayleigh and Raman scattering from optically active molecules. *Mol. Phys.*, **20**, 1111–1119.
Barron, L.D., Bogaard, M.P., and Buckingham, A.D. (1973a) Raman scattering of circularly polarized light by optically active molecules. *J. Am. Chem. Soc.*, **95**, 603–605.
Barron, L.D., Bogaard, M.P., and Buckingham, A.D. (1973b) Differential Raman scattering of right and left circularly polarized light by asymmetric molecules. *Nature*, **241**, 113–114.
Barron, L.D., Bogaard, M.P., and Buckingham, A.D. (1973c) Raman circular intensity differential observations on some monoterpenes. *J. Chem. Soc., Chem. Commun.*, 152–153.
Barron, L.D., and Vrbancich, J. (1983) On the sign convention for Raman optical activity. *Chem. Phys. Lett.*, **102**, 285–286.
Barron, L.D., and Escribano, J.R. (1985) Stokes Antistokes asymmetry in natural Raman optical activity. *Chem. Phys.*, **98**, 437–446.
Barron, L.D., Hecht, L., Hug, W., and MacIntosh, M.J. (1989) Backscattered Raman optical activity with CCD detector. *J. Am. Chem. Soc.*, **111**, 8731–8732.
Biot, J.B. (1815) *Bull. Soc. Philomath.*, 190.
Bosnick, B., Moskovits, M., and Ozin, G.A. (1972) Raman circular dichroism. Its observation in á-phenylethylamine. *J. Am. Chem. Soc.*, **94**, 4750–4751.
Bour, P., and Keiderling, T.A. (2005) Vibrational spectral simulation for peptides of mixed secondary structure: Method comparisons with the trpzip model hairpin. *J. Phys. Chem. B*, **109**, 23687–23697.
Brocki, T., Moskovits, M., and Bosnich, B. (1980) Vibrational optical activity. Circular differential Raman scattering from a series of chiral terpenes. *J. Am. Chem. Soc.*, **102**, 495–450.
Buckingham, A.D., Fowler, P.W., and Galwas, P.A. (1987) Velocity-dependent property surfaces and the theory of vibrational circular dichroism. *Chem. Phys.*, **112**, 1–14.
Bursi, R., Devlin, F.J., and Stephens, P.J. (1990) Vibrationally induced ring currents? The vibrational circular dichroism of methyl lactate. *J. Am. Chem. Soc.*, **112**, 9430–9432.
Che, D., Hecht, L., and Nafie, L.A. (1991) Dual and incident circular polarization Raman optical activity backscattering of ( − )-*trans*-pinane. *Chem. Phys. Lett.*, **180**, 182–190.
Cheng, J.C., Nafie, L.A., and Stephens, P.J. (1975) Polarization scrambling using a photoelastic modulator: Application to circular dichroism measurement. *J. Opt. Soc. Am.*, **65**, 1031–1035.
Chirgadze, Y.N., Venyaminov, S.Y., and Lobachev, V.M. (1971) Optical rotatory dispersion of polypeptides in the near-infrared region. *Biopolymers*, **10**, 809–820.
Cotton, A. (1895) *Compt. Rend.*, **120**, 989.
Deutsch, C.W., and Moscowitz, A. (1968) Optical activity of vibrational origin. I. A model helical polymer. *J. Chem. Phys.*, **49**, 3257–3272.
Deutsche, C.W., and Moscowitz, A. (1970) Optical activity of vibrational origin. II. Consequences of polymer conformation. *J. Chem. Phys.*, **53**, 2630–2644.
Devlin, F.J., Stephens, P.J., Cheeseman, J.R., and Frisch, M.J. (1996) Prediction of vibrational circular dichroism spectra using density functional theory: Camphor and fenchone. *J. Am. Chem. Soc.*, **118**, 6327–6328.
Devlin, R., and Stephens, P.J. (1987) Vibrational circular dichroism measurement in the frequency range of 800 to 650 $cm^{-1}$. *Appl. Spectrosc.*, **41**, 1142–1144.
Diem, M., Fry, J.L., and Burow, D.F. (1973) Circular differential Raman spectra of carvone. *J. Am. Chem. Soc.*, **95**, 253–255.

Ditchfield, R. (1974) A gauge-invariant LCAO method for N. M. R. chemical shifts. *Mol. Phys.*, **27**, 798–807.
Dutler, R., and Rauk, A. (1989) Calculated infrared absorption and vibrational circular dichroism intensities of oxirane and its deuterated analogues. *J. Am. Chem. Soc.*, **111**, 6957–6966.
Freedman, T.B., and Nafie, L.A. (1994) Theoretical formalism and models for vibrational circular dichroism intensity. In: *Modern Nonlinear Optics*, *Part 3* (eds M. Evans and S. Kielich), John Wiley & Sons, Inc., New York, pp. 207–263.
Freedman, T.B., Cao, X., Dukor, R.K., and Nafie, L.A. (2003) Absolute configuration determination of chiral molecules in the solution state using vibrational circular dichroism. *Chirality*, **15**, 743–758.
Frisch, M.J., Trucks, G.W., Schlegel, H.B. *et al.* (2003) Gaussian 03. Revision B. 03 ed. Gaussian, Inc., Pittsburgh, PA.
Frisch, M.J., Trucks, G.W., Schlegel, H.B. *et al.* (2009) Gaussian 09. Revision A. 1 ed. Gaussian, Inc., Wallingford, CT.
Galwas, P.A. (1983) Ph.D. thesis.University of Cambridge.
Guo, C., Shah, R.D., Dukor, R.K. *et al.* (2004) Determination of enantiomeric excess in samples of chiral molecules using Fourier transform vibrational circular dichroism spectroscopy: Simulation of real-time reaction monitoring. *Anal. Chem.*, **76**, 6956–6966.
Guo, C., Shah, R.D., Cao, X. *et al.* (2005) Enantiomeric excess determination by Fourier transform near-infrared vibrational circular dichroism spectroscopy: Simulation of real-time process monitoring. *Appl. Spectrosc.*, **59**, 1114–1124.
Gutowsky, H.S. (1951) Optical rotation of quartz in the infrared to 9.7 μ. *J. Chem. Phys.*, **19**, 438–441.
Haidinger, W. (1847) *Ann. Phys.*, **70**, 531.
Hecht, L., and Nafie, L.A. (1990) Linear polarization Raman optical activity: a new form of natural optical activity. *Chem. Phys. Lett.*, **174**, 575–582.
Hecht, L., Che, D., and Nafie, L.A. (1991) A new scattered circular polarization Raman optical activity instrument equipped with a charged coupled device detector. *Appl. Spectrosc.*, **45**, 18–25.
Hecht, L., and Nafie, L.A. (1991) Theory of natural Raman optical activity I. Complete circular polarization formalism. *Mol. Phys.*, **72**, 441–469.
Hecht, L., Che, D., and Nafie, L.A. (1992) Experimental comparison of scattered and incident circular polarization Raman optical activity in pinanes and pinenes. *J. Phys. Chem.*, **96**, 4266–4270.
Hecht, L., Phillips, A.L., and Barron, L.D. (1995) Determination of enantiomeric excess using Raman optical-activity. *J. Raman Spectrosc.*, **26**, 727–732.
Hediger, H.J., and Gunthard, H.H. (1954) Optical rotatory power of organic substances in the infrared. *Helv. Chim. Acta*, **37**, 1125–1133.
Herrmann, C., and Reiher, M. (2007) First principles approach to vibrational spectroscopy of biomolecules. *Top. Curr. Chem.*, **268**, 85–132.
Holzwarth, G., and Chabay, I. (1972) Optical activity of vibrational transitions. Coupled oscillator model. *J. Chem. Phys.*, **57**, 1632–1635.
Holzwarth, G., Hsu, E.C., Mosher, H.S. *et al.* (1974) Infrared circular dichroism of carbon–hydrogen and carbon–deuterium stretching modes. Observations. *J. Am. Chem. Soc.*, **96**, 251–252.
Hug, W. (1982) Instrumental and theoretical advances in Raman optical activity. In: *Raman Spectroscopy* (ed. J. Lascombe), John Wiley & Sons, Ltd, Chichester, pp. 3–12.
Hug, W. (2003) Virtual enantiomers as the solution of optical activity's deterministic offset problem. *Appl. Spectrosc.*, **57**, 1–13.
Hug, W., Kint, S., Bailey, G.F., and Scherer, J.R. (1975) Raman circular intensity differential spectroscopy. The spectra of (−)-a-pinene and (+)-a-phenylethylamine. *J. Am. Chem. Soc.*, **97**, 5589–5590.
Hug, W., and Surbeck, H. (1979) Vibrational Raman optical activity spectra recorded in perpendicular polarization. *Chem. Phys. Lett.*, **60**, 186–192.
Hug, W., and Hangartner, G. (1999) A very high throughput Raman and Raman optical activity spectrometer. *J. Raman Spectrosc.*, **30**, 841–852.
Jalkanen, K.J., and Stephens, P.J. (1988) Gauge dependence of vibrational rotational strengths: NHDT. *J. Phys. Chem.*, **92**, 1781–1785.
Katzin, L.I. (1964) Rotatory dispersion of quartz. *J. Phys. Chem.*, **68**, 2367–2370.
Keiderling, T.A., and Stephens, P.J. (1976) Vibrational circular dichroism in overtone and combination bands. *Chem. Phys. Lett.*, **41**, 46–48.

Lipp, E.D., Zimba, C.G., and Nafie, L.A. (1982) Vibrational circular dichroism in the mid-infrared using Fourier transform spectroscopy. *Chem. Phys. Lett.*, **90**, 1–5.

Lombardi, R.A., and Nafie, L.A. (2009) Observation and calculation of a new form of vibrational optical activity: Vibrational circular birefringence. *Chirality*, **21**, E277–E286.

London, F. (1937) Théorie quantique des courants interatomiques dans les combinaisons aromatiques. *J. Phys. Radium Paris*, **8**, 397–409.

Lowe, M.A., Segal, G.A., and Stephens, P.J. (1986a) The theory of vibrational circular dichroism: *trans*-1, 2-dideuteriocyclopropane. *J. Am. Chem. Soc.*, **108**, 248–256.

Lowe, M.A., Stephens, P.J., and Segal, G.A. (1986b) The theory of vibrational circular dichroism: *trans*-1, 2-dideuteriocyclobutane and propylene oxide. *Chem. Phys. Lett.*, **123**, 108–116.

Lowry, T.M. (1935) *Optical Rotatory Power*, Longmans, Green and Co., London.

Mason, S.F. (1973) The development of theories of optical activity and their applications. In: *Optical Rotatory Dispersion and Circular Dichroism* (eds F. Ciardelli and P. Salvadori), Heydon & Son, London, pp. 27–40.

Moskovits, M., and Gohin, A. (1982) Vibrational circular dichroism: Effect of charge fluxes and bond currents. *J. Phys. Chem.*, **86**, 3947–3950.

Nafie, L.A. (1983a) Adiabatic behavior beyond the Born–Oppenheimer approximation. Complete adiabatic wavefunctions and vibrationally induced electronic current density. *J. Chem. Phys.*, **79**, 4950–4957.

Nafie, L.A. (1983b) An alternative view on the sign convention of Raman optical activity. *Chem. Phys. Lett.*, **102**, 287–288.

Nafie, L.A. (1992) Velocity-gauge formalism in the theory of vibrational circular dichroism and infrared absorption. *J. Chem. Phys.*, **96**, 5687–5702.

Nafie, L.A. (1996) Theory of resonance Raman optical activity – the single electronic-state limit. *Chem. Phys.*, **205**, 309–322.

Nafie, L.A., Cheng, J.C., and Stephens, P.J. (1975) Vibrational circular dichroism of 2,2, 2-trifluoro-1-phenylethanol. *J. Am. Chem. Soc.*, **97**, 3842–3843.

Nafie, L.A., Keiderling, T.A., and Stephens, P.J. (1976) Vibrational circular dichroism. *J. Am. Chem. Soc.*, **98**, 2715–2723.

Nafie, L.A., and Walnut, T.H. (1977) Vibrational circular dichroism theory: A localized molecular orbital model. *Chem. Phys. Lett.*, **49**, 441–446.

Nafie, L.A., and Diem, M. (1979) Theory of high frequency differential interferometry: Application to infrared circular and linear dichroism via Fourier transform spectroscopy. *Appl. Spectrosc.*, **33**, 130–135.

Nafie, L.A., Diem, M., and Vidrine, D.W. (1979) Fourier transform infrared vibrational circular dichroism. *J. Am. Chem. Soc.*, **101**, 496–498.

Nafie, L.A., and Freedman, T.B. (1983) Vibronic coupling theory of infrared vibrational intensities. *J. Chem. Phys.*, **78**, 7108–7116.

Nafie, L.A., Oboodi, M.R., and Freedman, T.B. (1983) Vibrational circular dichroism in amino acids and peptides. 8. A chirality rule for the methine C*H stretching mode. *J. Am. Chem. Soc.*, **105**, 7449–7450.

Nafie, L.A., and Freedman, T.B. (1986) The ring current mechanism of vibrational circular dichroism. *J. Phys. Chem.*, **90**, 763–767.

Nafie, L.A., and Freedman, T.B. (1989) Dual circular polarization Raman optical activity. *Chem. Phys. Lett.*, **154**, 260–266.

Nafie, L.A., and Che, D. (1994) Theory and measurement of Raman optical activity. In: *Modern Nonlinear Optics, Part 3* (eds M. Evans, and S. Kielich), John Wiley & Sons, Inc., New York, pp. 105–149.

Nafie, L.A., Brinson, B.E., Cao, X. *et al.* (2007) Near-infrared excited Raman optical activity. *Appl. Spectrosc.*, **61**, 1103–1106.

Nafie, L.A., and Dukor, R.K. (2007) Pharmaceutical applications of vibrational optical activity. In: *Applications of Vibrational Spectroscopy in Pharmaceutical Research and Development* (eds. D. Pivonka, P.R. Griffiths, and J.M. Chalmers), John Wiley & Sons, Ltd., Chichester, pp. 129–154.

Osborne, G.A., Cheng, J.C., and Stephens, P.J. (1973) Near-infrared circular dichroism and magnetic circular dichroism instrument. *Rev. Sci. Instrum.*, **44**, 10.

Polavarapu, P.L. (1990) *Ab initio* Raman and Raman optical activity spectra. *J. Phys. Chem.*, **94**, 8106–8112.

Polavarapu, P.L., and Deng, Z.Y. (1996) Measurement of vibrational circular-dichroism below $\sim 600\,\mathrm{cm}^{-1}$: Progress towards meeting the challenge. *Appl. Spectrosc.*, **50**, 686–692.

Qu, X., Lee, E., Yu, G.S. *et al.* (1996) Quantitative comparison of experimental infrared and Raman optical-activity spectra. *Appl. Spectrosc.*, **50**, 649–657.

Russel, M.I., Billardon, M., and Badoz, J.P. (1972) Circular and linear dichrometer for the near infrared. *Appl. Opt.*, **11**, 2375–2378.

Schellman, J.A. (1973) Vibrational optical activity. *J. Chem. Phys.*, **58**, 2882–2886.

Schweitzer-Stenner, R., Measey, T., Kakalis, L. *et al.* (2007) Conformations of alanine-based peptides in water probed by FTIR, Raman, vibrational circular dichroism, electronic circular dichroism, and NMR spectroscopy. *Biochemistry*, **46**, 1587–1596.

Shanmugam, G., and Polavarapu, P.L. (2005) Film techniques for vibrational circular dichroism measurements. *Appl. Spectrosc.*, **59**, 673–681.

Spencer, K.M., Freedman, T.B., and Nafie, L.A. (1988) Scattered circular polarization Raman optical activity. *Chem. Phys. Lett.*, **149**, 367–374.

Spencer, K.M., Cianciosi, S.J., Baldwin, J.E. *et al.* (1990) Determination of enantiomeric excess in deuterated chiral hydrocarbons by vibrational circular dichroism spectroscopy. *Appl. Spectrosc.*, **44**, 235–238.

Stephens, P.J., and Clark, R. (1979) Vibrational circular dichroism: The experimental viewpoint. In: *Optical Activity and Chiral Discrimination* (ed. S. F. Mason), D. Reidel, Dordrecht, pp. 263–287.

Stephens, P.J. (1985) Theory of vibrational circular dichroism. *J. Phys. Chem.*, **89**, 748–752.

Stephens, P.J., Chabalowski, C.F., Devlin, F.J., and Jalkanen, K.J. (1994) *Ab initio* calculation of vibrational circular-dichroism spectra using large basis-set MP2 force-fields. *Chem. Phys. Lett.*, **225**, 247–257.

Stephens, P.J., and Devlin, F.J. (2000) Determination of the structure of chiral molecules using *ab initio* vibrational circular dichroism spectroscopy. *Chirality*, **12**, 172–179.

Su, C.N., Heintz, V.J., and Keiderling, T.A. (1980) Vibrational circular dichroism in the mid-infrared. *Chem. Phys. Lett.*, **73**, 157–159.

Vargek, M., Freedman, T.B., Lee, E., and Nafie, L.A. (1998) Experimental observation of resonance Raman optical activity. *Chem. Phys. Lett.*, **287**, 359–364.

West, C.D. (1954) Anomalous rotatory dispersion of quartz above 3.7 μ. *J. Chem. Phys.*, **22**, 749–750.

Wyss, H.R., and Gunthard, H.H. (1966) Diphenyl-dinaphto-(2′,1′:1,2;1″, 2″:3,4)-5,8-diaza-cyclooctatetraen (I) und 3′,6″-Dimethyl-1,2:3,4-dibenz-1,3-cycloheptadien-6-on (II) im Infrarot. *Helv. Chim. Acta*, **49**, 660–663.

Yu, G.-S., and Nafie, L.A. (1994) Isolation of preresonance and out-of-phase dual circular polarization Raman optical activity. *Chem. Phys. Lett.*, **222**, 403–410.

Zuber, G., and Hug, W. (2004) Rarefied basis sets for the calculation of optical tensors. 1. The importance of gradients on hydrogen atoms for the Raman scattering tensor. *J. Phys. Chem. A*, **108**, 2108–2118.